



1 **Toward a typology of river functioning: a**  
2 **comprehensive study of POM composition at multi-**  
3 **rivers scale**

4

5 Ferchiche Florian<sup>1</sup>, Liénart Camilla<sup>1</sup>, Charlier Karine<sup>1</sup>, Deborde Jonathan<sup>2,3</sup>, Giraud Mélanie<sup>4</sup>,  
6 Kerhervé Philippe<sup>5</sup>, Polsenaere Pierre<sup>1,3</sup>, Savoye Nicolas<sup>1\*</sup>

7 <sup>1</sup> Univ. Bordeaux, CNRS, EPHE, Bordeaux INP, UMR 5805 EPOC, F-33600 Pessac, France

8 <sup>2</sup> Univ. Pau & Pays Adour, CNRS, E2S UPPA – MIRA, UMR 5254 IPREM, F-64000 Pau, F-64600 Anglet, France

9 <sup>3</sup> Ifremer, COAST, F-17390 La Tremblade, France

10 <sup>4</sup> MNHN, CRESCO, Station Marine de Dinard, F-35800 Dinard, France

11 <sup>5</sup> Univ. Perpignan, CNRS, UMR 5110 CEFREM, F-66860 Perpignan, France

12

13 \*Correspondence to: Nicolas Savoye ([nicolas.savoye@u-bordeaux.fr](mailto:nicolas.savoye@u-bordeaux.fr)) (+33)556223916

14 Université de Bordeaux - UMR 5805 EPOC - Station marine d'Arcachon - 2 rue du Professeur Jolyet - 33120  
15 Arcachon

16

17 **Keywords:** river-estuary interface; particulate organic matter; stable isotopes; multi-ecosystems  
18 **study.**



## 19 **Abstract**

20 In riverine systems, particulate organic matter (POM) originates from various sources, each  
21 having its proper dynamics related to production, decomposition, transport and burial. There is  
22 a significant amount of spatiotemporal heterogeneity in the POM pool. The current study, based  
23 on C and N elemental and isotopic ratios, applies Bayesian mixing models associated with  
24 statistical multivariate analyses to 1) quantify and examine relationships between POM  
25 composition and environmental forcings, and 2) draw a typology of river functioning based on  
26 POM composition and its seasonal dynamics. Twenty-three rivers of temperate climate  
27 accounting for a large diversity of environmental conditions were sampled fortnightly to  
28 monthly for one to seven years at the River-Estuary Interface (REI). Phytoplankton and labile  
29 terrestrial material were present in all rivers, contrary to sewage and refractory terrestrial  
30 material that were present in only a few. At the twenty-three studied rivers scale, POM sources  
31 are strongly related to watershed characteristics, phytoplankton being associated with  
32 agricultural surfaces and labile terrestrial material to soil organic carbon content and erosion  
33 rate. Overall, seasonal variations of phytoplankton, labile and refractory terrestrial material  
34 were mainly related to drivers of phytoplankton growth, river flow, and sediment resuspension,  
35 respectively. A statistical regionalization defined four river types: (1) systems whose POM is  
36 dominated by labile terrestrial material all year long; (2) systems whose POM is composed of  
37 labile and refractory terrestrial material, in addition to phytoplankton, with variable seasonality  
38 according to rivers; systems whose POM is composed of phytoplankton and labile terrestrial  
39 material (3) without and (4) with pronounced seasonality.

40 This work offers a comprehensive understanding of POM composition, dynamics and drivers  
41 at the REI in temperate climates, complementing similar work dedicated to coastal systems.  
42 Future work dedicated to estuaries is called to get a comprehensive understanding of POM  
43 composition, dynamics and drivers along the Land-Ocean Aquatic Continuum.

44 This study examines particulate organic matter (POM) composition and dynamics in 23  
45 temperate rivers. Carbon and nitrogen isotope analysis revealed four river types based on  
46 dominant POM sources (phytoplankton, terrestrial material). Watershed characteristics  
47 influence POM composition while seasonal variations in river flow and sediment resuspension  
48 drive POM dynamics. This study improves the understanding of river systems and calls for  
49 further studies exploring downstream estuarine functioning.



## 50 **1. Introduction**

51 The River-Estuary Interface (REI) is a crucial biogeochemical interface for understanding the  
52 transition between continental and coastal systems, beginning at estuaries, because of its key  
53 location within the Land-Ocean Aquatic Continuum (LOAC) (Bate et al., 2002). Indeed, rivers  
54 then estuaries are important filters for matters received from land, transporting and transforming  
55 organic matter and nutrients along their courses (Bouwman et al., 2013; Dürr et al., 2011;  
56 Middelburg and Herman, 2007). These processes are fundamental in understanding global  
57 biogeochemical cycles (Regnier et al., 2013), as these matters directly fuel coastal ocean trophic  
58 networks (Dagg et al., 2004). However, in a Human-impacted world, anthropogenic activities  
59 and disturbances can modify natural matter fluxes. For example, damming rivers directly  
60 impacts nutrient flows (Wang et al., 2022) and sediment transportation (Kang et al., 2021).  
61 Indirectly, land use in river basins can lead to changes in the river matter quality (Lambert et  
62 al., 2017).

63 In aquatic systems, particulate organic matter (POM), i.e., non-mineral particles, is composed  
64 of different sources that originate from different compartments: phytoplankton, macrophytes  
65 from the aquatic systems as well as soil particles and plant litter from terrestrial compartments  
66 and even treated and untreated anthropogenic organic matter (Ke et al., 2019; Sun et al., 2021;  
67 Zhang et al., 2021). Depending on its composition, POM exhibits different levels of lability,  
68 i.e., different levels of biogeochemical reactivity and bioavailability. For instance,  
69 phytoplankton is usually considered mainly labile and thus highly biogeochemically reactive  
70 and bioavailable for primary consumers, while terrestrial POM is usually considered mainly  
71 refractory and thus lightly biogeochemically reactive and poorly bioavailable for the food webs  
72 (Brett et al., 2017; David et al., 2005; Etcheber et al., 2007). In other words, the determination  
73 and quantification of POM composition (i.e., the relative proportion of each source composing  
74 the POM) allow a better understanding of biogeochemical cycles and trophic ecology in aquatic  
75 systems (e.g., Grunicke et al., 2023; Minaudo et al., 2016). Nevertheless, POM composition  
76 and concentration are not only involved in biogeochemical and biological processes (e.g.,  
77 primary production, remineralization, feeding) but undergo other processes inside and at the  
78 interface of the aquatic compartment (Canuel and Hardison, 2016). River hydrodynamics is one  
79 of the main drivers of POM composition and concentration, leading to great variabilities in  
80 terrestrial material quality and quantity (Dalzell et al., 2007; Lebreton et al., 2016; Marshall et  
81 al., 2021), possibly leading to changes in source origins (Arellano et al., 2019; Barros et al.,  
82 2010). Also, changes in anthropic pressures can change POM composition and concentration  
83 and their seasonal variations, like a decrease in nutrient load (Minaudo et al., 2015).

84 This dependency of POM composition and concentration on physical, biogeochemical and  
85 biological processes and their responses to environmental conditions and characteristics (Bonin  
86 et al., 2019; Falkowski et al., 1998; Field et al., 1998; Galeron et al., 2017; Goñi et al., 2009;



87 Lebreton et al., 2016) may lead to distinguishing different typology of rivers, i.e., the likeliness  
88 of rivers to carry preferential sources. For instance, highly turbid systems are more likely to  
89 carry refractory materials (Savoye et al., 2012), while eutrophicated rivers carry high biomass  
90 of phytoplankton (Hounshell et al., 2022; Minaudo et al., 2015) and contrasted processes can  
91 lead to a mixture between different detrital sources, as soil matter vs. fresh terrestrial plants  
92 (Ogrinc et al., 2008). However, to date, no study clearly determined typologies of rivers based  
93 on POM composition and its seasonal variability.

94 To distinguish POM sources and quantify their contribution to POM composition, different  
95 tools such as elemental and isotopic ratios, pigments or specific compounds like fatty acids or  
96 alkanes can be used (e.g., Chevalier et al., 2015; Liénart et al., 2020, 2017; Savoye et al., 2012).  
97 Elemental and isotopic ratios are usually considered robust and allow the quantification of POM  
98 composition in this kind of study (e.g., Liénart et al., 2016; Onstad et al., 2000; Wang et al.,  
99 2021). Indeed, they usually allow the discrimination of, e.g., riverine phytoplankton, terrestrial  
100 POM and wastewater POM (Ke et al., 2019) and they can be used for running mixing models  
101 that quantify the proportion of the different sources into a POM mixture (Parnell et al., 2013).  
102 However, studies using mixing models for quantifying POM composition in river systems are  
103 still scarce (e.g., Ferchiche et al., 2025, 2024; Kelso and Baker, 2022, 2020; Zhang et al., 2021).

104 Within the scope of better understanding the role of the LOAC in modifying matter fluxes and  
105 quality, the present study gathered published data and results from 23 rivers at the river-estuary  
106 interface with the aim of 1) quantifying the POM composition each river, 2) describing the  
107 seasonal variations of this composition, 3) determining the drivers of the seasonal variability  
108 within each river and the spatial variability among the 23 rivers, and then 4) determining a  
109 typology of rivers according to their POM composition and dynamics. This study is the first to  
110 precisely quantify POM composition in numerous and various temperate river systems and  
111 classify river types according to POM composition and dynamics.

## 112 **2. Material and methods**

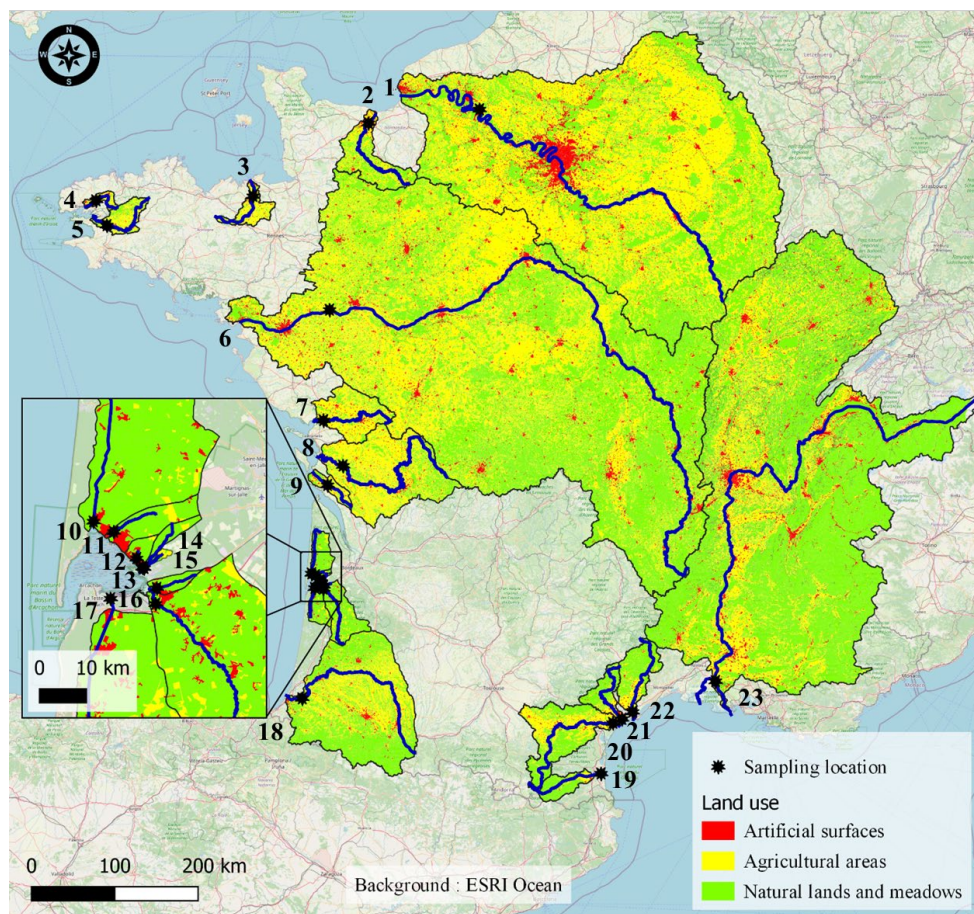
113 Twenty-three temperate rivers were studied at their river-estuary interface (i.e., right upstream  
114 of the tidal influence). All the data come from published studies or national open databases. To  
115 minimize the heterogeneity of the datasets in terms of sampling strategy, we have considered  
116 for this study the datasets only when 1) C/N ratio along with isotopic ratio of carbon and/or  
117 nitrogen were available, 2) particulate matter characteristics like, suspended particulate matter  
118 (SPM), particulate organic carbon (POC), particulate nitrogen (PN), chlorophyll *a* (chl *a*) were  
119 also available, 3) datasets exhibited at least a monthly temporal resolution for one full year.  
120 When needed, published datasets were completed and harmonized thanks to national databases.

### 121 **2.1. Study sites**



122 The studied rivers and associated watersheds are all located in France (except the upper basin  
123 of the Rhône River) and distributed in all regions of the mainland. Three, fifteen and five of  
124 these rivers flow into the English Channel, the Atlantic Ocean and the Mediterranean Sea (Fig.  
125 1). They encompass large gradients of environmental characteristics (Tab. 1). For instance, the  
126 Loire River is one of the largest in Europe (length: 1006 km; watershed: 117,356 km<sup>2</sup>), while  
127 the littlest studied river is a very small stream of the Arcachon lagoon (length: 3 km; watershed:  
128 18 km<sup>2</sup>). They encompass large gradients of river flow (annual mean: 0.3 m<sup>3</sup>/s – 1572 m<sup>3</sup>/s),  
129 turbidity (SPM annual mean: 2.7 mg/l – 40.9 mg/l) and trophic status (from oligotrophic to  
130 eutrophic rivers; chl *a* annual mean: 0.4 µg/l – 57.1 µg/l). At last, they undergo a gradient of  
131 anthropic pressures as illustrated by the proportion of artificial surfaces (0.1 % – 5.6 %) and  
132 agricultural areas (0 % – 86 %) in the watersheds (Fig. 1).

133



134

135 Figure 1 Studied rivers (thick blue lines), sampling locations (black stars) and watersheds (thin  
136 black lines) including the main land uses (red, yellow and green colors). 1: Seine; 2: Orne; 3:



137 Rance; 4: Elorn; 5: Aulne; 6: Loire; 7: Sèvre niortaise; 8: Charente; 9: Seudre; 10: Canal du  
138 Porge; 11: Cirès; 12: Milieu; 13: Lanton; 14: Renet; 15: Tagon; 16: Leyre; 17: Canal des  
139 Landes; 18: Adour; 19: Têt; 20: Aude; 21: Orb; 22: Hérault; 23: Rhône.



140 **Table 1** Overview of river samplings and characteristics. Values are given as annual mean over the study period for river flow, temperature,  
 141 suspended particulate matter (SPM) and chlorophyll *a* (chl *a*). Id.: identification number; Number: number of sampling dates. River types were  
 142 defined within the scope of the present study (see section 3.4).

River Id	River type	Sampled period	Sampling Periodicity	Num ber	Latitude	Longitude	River length (km)	Catchment area (km <sup>2</sup> )	River flow (m <sup>3</sup> /s)	Water temperature (°C)	SPM (mg/l)	Chl <i>a</i> (µg/l)	References
Seine 1	IV	06/2014 to 06/2015	monthly	13	49.3067	1.2425	774	79000	496	15.0	21	2.8	Liénard et al., 2017, 2018
Orne 2	III	06/2014 to 06/2015	monthly	13	49.1797	-0.3491	169	2932	16	14.5	11	1.8	Liénard et al., 2017, 2018
Rance 3	IV	06/2014 to 05/2015	monthly	12	48.4916	-2.0014	103	1195	1.37	15.1	21	57.1	Liénard et al., 2017, 2018
Elorn 4	IV	01/2014 to 06/2015	monthly	17	48.4505	-4.2483	56	385	6	12.3	16	3.0	Liénard et al., 2017, 2018
Aulne 5	IV	01/2014 to 06/2015	monthly	17	48.2127	-4.0944	144	1875	30	14.4	7	3.3	Liénard et al., 2017, 2018
Loire 6	IV	10/2009 to 07/2012	bi-monthly	67	47.3920	-0.8604	1006	117356	630	14.1	19	18.7	Ferchiche et al., 2024
Sèvre 7	IV	03/2014 to 03/2015	monthly	13	46.3153	-1.0039	158	3650	3.72	15.7	13	3.8	Liénard et al., 2017, 2018
Charente 8	III	03/2014 to 09/2015	monthly	13	45.8680	-0.7131	381	9855	68	15.1	13	1.3	Liénard et al., 2017, 2018
Seudre 9	I	03/2014 to 09/2015	monthly	15	45.6740	-0.9331	68	855	1.81	14.3	17	0.5	Liénard et al., 2017, 2018
Porge 10	III	01/2008 to 02/2009	monthly	14	44.7898	-1.1612	57	222	3.48	13.3	12	5.0	Polsenaere et al., 2013
Chères 11	I	02/2008 to 02/2009	monthly	13	44.7598	-1.1107	12	45	0.58	12.2	5	0.4	Polsenaere et al., 2013
Renet 12	I	02/2008 to 02/2009	bi-monthly	23	44.7144	-1.0441	3	18	0.56	12.9	10	0.6	Polsenaere et al., 2013
Lanton 13	I	02/2008 to 02/2009	monthly	13	44.7002	-1.0244	15	36	0.26	12.5	11	1.2	Polsenaere et al., 2013
Milieu 14	I	02/2008 to 02/2009	monthly	13	44.6973	-1.0225	7	21	0.58	12.7	7	0.4	Polsenaere et al., 2013
Tagon 15	I	02/2008 to 02/2009	bi-monthly	26	44.6590	-0.9891	10	30	0.64	12.6	13	1.3	Polsenaere et al., 2013
Leyre 16	I	01/2008 to 03/2010 and 02/2014 to 02/2015	bi-monthly or monthly	59	44.6263	-0.9961	116	1700	17	13.0	11	0.9	Dubois et al., 2012 / Polsenaere et al., 2013 / Liénard et al., 2017, 2018
Landes 17	III	02/2008 to 02/2009	monthly	12	44.6169	-1.1091	14	117	0.49	14.1	3	1.1	Polsenaere et al., 2013
Adour 18	III	04/2013 to 06/2014 and 05/2017 to 05/2017	monthly	24	43.4988	-1.2949	308	16912	516	14.0	48	2.4	Liénard et al., 2016 / Deborde, 2019
Têt 19	II	01/2006 to 05/2010	monthly	52	42.7137	2.9935	115	1369	23	15.7	8	NA	Higuens et al., 2014
Hérault 20	II	01/2006 to 05/2010	monthly	52	43.3594	3.4354	148	2582	53	16.0	7	NA	Higuens et al., 2014
Orb 21	II	01/2006 to 05/2010	monthly	52	43.2850	3.2813	136	1585	23	15.7	8	NA	Higuens et al., 2014
Aude 22	II	01/2006 to 05/2010	monthly	52	43.2442	3.1527	223	5327	40	14.2	31	NA	Higuens et al., 2014
Rhône 23	II	12/2003 to 01/2011	monthly	105	43.6787	4.6212	812	95590	1572	15.9	41	1.9	Hammelin-Vivien et al., 2010 / Cathalat et al., 2013 / Higuens et al., 2014

143



## 144 2.2. Data origin

145 Regarding the core parameters (C/N ratio,  $\delta^{13}\text{C}$ ,  $\delta^{15}\text{N}$ , water temperature, SPM, POC, PN, chl  
146 *a*), most of the data sets come from published studies (Canton et al., 2012; Cathalot et al., 2013;  
147 Dubois et al., 2012; Ferchiche et al., 2024; Harmelin-Vivien et al., 2010; Higuera et al., 2014;  
148 Liénart et al., 2016, 2017, 2018; Polsenaere et al., 2013), while most of additional parameters  
149 come from national databases (Tab. A1). When not available in the cited studies, concentrations  
150 of SPM,  $\text{NO}_3^-$ ,  $\text{NH}_4^+$  and  $\text{PO}_4^{3-}$ , pH and water temperature were retrieved from the *Naiades*  
151 database (<https://naiades.eaufrance.fr/>, consulted the 07/10/2023). Note that these parameters  
152 were not necessarily measured or sampled exactly at the same location or date for *Naiades* than  
153 in the cited studies. In that case, the location was chosen as close as possible to the study  
154 location and data values were time-interpolated to match the study date. Meteorological  
155 variables (air temperature, zonal and meridional wind, irradiance) come from Météo France,  
156 the French meteorological service. Wind data was received originally as direction and speed.  
157 To remove the angular bias, they were combined using scalar products to get zonal and  
158 meridional wind speeds, which range between minus and plus infinity (see Lheureux et al.,  
159 2022, for more details). River flows were retrieved from the *Banque Hydro* database  
160 (<https://www.hydro.eaufrance.fr/>, consulted the 07/10/2023) or from Polsenaere et al. (2013)  
161 for the small streams. Land use proportions originate from the national Corine Land Cover  
162 database (<https://www.statistiques.developpement-durable.gouv.fr/corine-land-cover-0>,  
163 consulted the 10/01/2024). Soil organic carbon data originate from the SoilTrEC database  
164 ([https://esdac.jrc.ec.europa.eu/content/predicted-distribution-soc-content-europe-based-lucas-  
165 biosoil-and-czo-context-eu-funded-1](https://esdac.jrc.ec.europa.eu/content/predicted-distribution-soc-content-europe-based-lucas-biosoil-and-czo-context-eu-funded-1), consulted the 10/01/2024). Net erosion soil data  
166 originates from the WaTEM/SEDEM database ([https://esdac.jrc.ec.europa.eu/content/estimate-  
167 net-erosion-and-sediment-transport-using-watemsedem-european-union](https://esdac.jrc.ec.europa.eu/content/estimate-net-erosion-and-sediment-transport-using-watemsedem-european-union), consulted the  
168 10/01/2024).

169 It should be noted that a complete study was already dedicated to the Loire River and reported  
170 as a companion article (Ferchiche et al., 2024). Consequently, the results are not reported in the  
171 present study but are used for multi-system comparisons (Fig. 5 and 7, and corresponding text).

## 172 2.3. Determination of sources signatures

173 To run mixing models for quantifying POM composition, it is previously needed to 1)  
174 determine sources of POM, and 2) associate elemental and isotopic signatures to these sources.  
175 In riverine systems, phytoplankton and terrestrial POM are the main sources that are usually  
176 considered as fueling the POM (e.g., Ferchiche et al., 2024; Pradhan et al., 2016; Sarma et al.,  
177 2014). Nevertheless, sewage POM may also contribute (Higuera et al., 2014). Consequently,  
178 phytoplankton, terrestrial POM and sewage POM were considered as potential sources in this  
179 study.





180 Phytoplankton cannot be easily picked up from bulk particles to measure its elemental and  
181 isotopic ratios. Therefore, the method developed and used by Savoye et al. (2012), Liénart et  
182 al. (2017) and Ferchiche et al. (2024) was applied here. It consists of determining the elemental  
183 and isotopic ratios from a subset of the bulk dataset. Briefly, phytoplankton-dominated POM is  
184 characterized by a low POC/chl *a* ratio ( $\leq 200$  or even  $\leq 100$  g/g; Savoye et al., 2003 and  
185 references therein). Thus, elemental and isotopic ratios of samples exhibiting a low POC/chl *a*  
186 ratio can be considered as good estimates of phytoplankton elemental and isotopic ratios. When  
187 the POC/chl *a* ratio is not available, samples exhibiting a high PN/SPM ratio can be used.  
188 Additional constraints may be used to minimize potential overlap between phytoplankton and  
189 terrestrial elemental and isotopic signatures. Phytoplankton elemental and especially isotopic  
190 ratios may deeply vary over time and space depending on primary production intensity and  
191 potential limiting factors, nutrient origin, etc. (e.g., Miller et al., 2013; Savoye et al., 2003).  
192 When existing, this variability has to be taken into account to avoid using elemental and isotopic  
193 signatures that are not valid at the time or location of the sampling. This could be performed by  
194 using regressions between elemental and/or isotopic ratios and environmental variables (see  
195 Ferchiche et al., 2024; Liénart et al., 2017; Savoye et al., 2012). At last, when no samples exhibit  
196 a low POC/chl *a* ratio, samples exhibiting the lowest (even if high) POC/chl *a* ratios can be  
197 used but the data should be firstly corrected from the contribution of the terrestrial POM using  
198 Equations 1-3.

$$199 \delta^{13}\text{C}_{\text{sample}} = ([\text{POC}]_{\text{phytoplankton}} \times \delta^{13}\text{C}_{\text{phytoplankton}} + [\text{POC}]_{\text{terrestrial}} \times \delta^{13}\text{C}_{\text{terrestrial}}) / [\text{POC}]_{\text{sample}} \quad (\text{eq. 1})$$

$$201 [\text{POC}]_{\text{phytoplankton}} = [\text{chl } a]_{\text{sample}} \times (\text{POC/chl } a)_{\text{mean}} \quad (\text{eq. 2})$$

$$202 [\text{POC}]_{\text{terrestrial}} = [\text{POC}]_{\text{sample}} - [\text{POC}]_{\text{phytoplankton}} \quad (\text{eq. 3})$$

203 where  $(\text{POC/chl } a)_{\text{mean}}$  is the mean POC/chl *a* ratio of the samples used to determine  
204 phytoplankton signatures. Similar equations are used for the N/C ratio,  $\delta^{15}\text{N}$  and C/N ratio but  
205 using PN instead of POC for  $\delta^{15}\text{N}$  and C/N ratio.

206 Elemental and isotopic signatures of terrestrial POM can be estimated by directly measuring  
207 elemental and isotopic ratios in terrestrial materials like soil and vascular plants (e.g., Sarma et  
208 al., 2014). However, this does not take into account the reworking of this material within the  
209 river system which can affect these signatures (Hou et al., 2021). Thus, similarly to  
210 phytoplankton, elemental and isotopic signatures of terrestrial POM can be estimated using  
211 subsets of bulk data, following the approach of Savoye et al. (2012), Liénart et al. (2017) and  
212 Ferchiche et al. (2025, 2024). Terrestrial POM is usually characterized by high POC/chl *a* and  
213 C/N ratios and low POC/SPM ratios (Etcheber et al., 2007; Savoye et al., 2003 and references  
214 therein). However, during its decay in aquatic systems, terrestrial POM is colonized by bacteria  
215 (low C/N ratio) resulting in a consortium terrestrial POM + bacteria of lower C/N ratio than the  
216 original terrestrial POM (Etcheber et al., 2007; Savoye et al., 2012). Finally, one can



217 discriminate two kinds of terrestrial POM: refractory terrestrial POM characterized by high  
218 POC/chl *a* and C/N ratios and very low POC/SPM ratio, and quite labile terrestrial POM  
219 characterized by high POC/chl *a* ratio, intermediate C/N ratios and low POC/SPM ratio  
220 (Etcheber et al., 2007; Savoye et al., 2012). Thus, subsets of high POC/chl *a* ratio can be  
221 selected to determine the elemental and isotopic signatures of terrestrial POM. The C/N ratio  
222 can be used to discriminate labile from refractory terrestrial POM. When no samples exhibit a  
223 high POC/chl *a* ratio, samples exhibiting the highest (even if quite low) POC/chl *a* ratio can be  
224 used but the data should be firstly corrected from the contribution of the phytoplankton POM  
225 using Equations 1-3.

226 Elemental and isotopic ratios of riverine POM can exhibit a departure from a simple  
227 phytoplankton-terrestrial POM mixing. In the present study, this was the case in only two rivers.  
228 For the Têt River, elemental and isotopic signature of anthropogenic POM was available in  
229 Higueras et al. (2014). It consisted of analyses of POM sampled in the wastewater treatment  
230 plant (WWTP) the closest to the sampling site. For the Orb River, the signatures were estimated  
231 using the sample exhibiting the lowest  $\delta^{15}\text{N}$ , typical of anthropogenic POM (Ke et al., 2019).

232 The estimation of POM-source signatures was performed independently for each river, except  
233 for some of the tributaries of the Arcachon Lagoon (rivers 11 to 15), where data sets were  
234 gathered, thanks to very similar characteristics (same  $\delta^{13}\text{C}$  of dissolved inorganic carbon;  
235 Polsenaere et al., 2013), to get a larger subset of data for estimating elemental and isotopic  
236 signatures more accurately. All criteria used for defining the above-described subsets are  
237 reported in Table 2.

238 Table 2 Elemental and isotopic signatures of POM sources and criteria used to choose the data  
239 subset to determine them. When the signature did not vary over time, average  $\pm$  standard  
240 deviation are reported. When the signature did vary over time, minimum and maximum values,  
241 standard deviations as well as equations are reported. The types of mixing models performed  
242 for each river are also indicated (carbon mixing models were performed using  $\delta^{13}\text{C}$  and N/C  
243 ratio or only  $\delta^{13}\text{C}$ ; nitrogen mixing models were performed using  $\delta^{15}\text{N}$  and C/N ratio; mixed  
244 mixing models were performed using  $\delta^{13}\text{C}$ ,  $\delta^{15}\text{N}$  and N/C ratio). POC% (or PN%) = Particulate  
245 Organic Carbon (or Particulate Nitrogen) to Suspended Particulate Matter ratio (%); C/N =  
246 POC/PN ratio (mol/mol); chl *a* = chlorophyll *a* ( $\mu\text{g/l}$ ); phaeo = phaeopigments ( $\mu\text{g/l}$ ); conduc =  
247 conductivity ( $\mu\text{S}$ ); temp = water temperature ( $^{\circ}\text{C}$ ); Q7 = mean of past seven days river flow;  
248  $\text{NO}_3^-$  = nitrate ( $\text{mg}(\text{NO}_3^-)/\text{l}$ ).



River	Source discriminants				Model performed			Labile terrestrial matter				Refractory terrestrial matter			
	Labile terrestrial matter	Refractory terrestrial matter	Phytoplankton	WWTP's POM	Carbon	Nitrogen	Mixed	$\delta^{13}\text{C}$	$\delta^{15}\text{N}$	C/N	N/C	$\delta^{13}\text{C}$	$\delta^{15}\text{N}$	C/N	N/C
Seine	C/N > 10		POC/chla < 200		X	X		-28.5 ± 0.3	6.6 ± 0.9	10.6 ± 0.3	0.093 ± 0.002				
Orne	C/N > 11		POC/chla < 500		X	X		-28.4 ± 0.3	5.8 ± 1.0	12.4 ± 0.4	0.082 ± 0.003				
Rance	POC/chla > 200 and chla < 10		POC/chla < 150		X	X		-26.8 ± 0.2	6.1 ± 0.7	8.8 ± 0.4	0.113 ± 0.007				
Elorn	C/N > 12		POC/chla < 200		X	X		-28.4 ± 0.7	5.8 ± 0.9	13.0 ± 0.8	0.077 ± 0.005				
Aulne	C/N > 11		POC/chla < 200 and C/N < 9		X	X		-28.9 ± 0.8	5.8 ± 0.8	12.1 ± 1.1	0.08 ± 0.008				
Loire	POC/chla > 500		POC/chla < 200		X	X		-28.1 ± 0.1	5.9 ± 0.3	10.3 ± 0.2	0.097 ± 0.002				
Sèvre Niortaise	C/N > 14		POC/chla < 300		X			-28.0 ± 0.4			0.057 ± 0.040				
Charente	C/N > 12		POC/chla < 300		X	X		-29.0 ± 0.4	4.7 ± 0.2	14.5 ± 0.5	0.069 ± 0.002				
Seudre	POC/chla > 2000 and C/N > 12		POC/chla < 1000		X			-28.5 ± 0.1							
Porge	C/N > 15		$\delta^{13}\text{C}$ : POC/chla < 100 ; N/C : mean of Cirès to Landes		X			-26.5 ± 1.1			0.050 ± 0.007				
Cirès / Renet / Milieu / Lanton / Tagon	C/N > 15 and chla < 1		POC/chla < 1000 and POC% > 10		X			-28.5 ± 0.5			0.053 ± 0.013				
Leyre	C/N > 15 and chla < 1		POC/Chla < 1000, $\delta^{13}\text{C}$ < 28.59 and POC% > 10		X			-28.3 ± 0.5			0.06 ± 0.005				
Landes	C/N > 12		POC/Chla < 600, $\delta^{13}\text{C}$ < -29.1		X			-29.1 ± 0.4			0.075 ± 0.002				
Adour	POC/chla > 3000		POC/chla < 200		X			-26.0 ± 0.9			0.099 ± 0.008				
Têt	C/N > 11.5	POC% < 4.25	PN% > 2, $\delta^{13}\text{C}$ < 26 and $\delta^{15}\text{N}$ > 5	Measured		X		-26.0 ± 0.2	3.7 ± 0.6	12.2 ± 0.5	0.082 ± 0.002	-26.0 ± 0.6	6.7 ± 1.4	5.8 ± 1.4	0.180 ± 0.045
Aude	C/N > 12	Q7 > 70	PN% > 1 or 2 and C/N < 6			X		-28.1 ± 0.6	6.3 ± 0.1	15.3 ± 1.6	0.066 ± 0.007	-28.0 ± 0.7	4.7 ± 0.4	7.3 ± 1.0	0.139 ± 0.018
Orb	C/N > 10		PN% > 2, $\delta^{15}\text{N}$ > 4.06	Lower $\delta^{15}\text{N}$		X		-27.1 ± 0.4	3.7 ± 0.4	10.5 ± 0.3	0.095 ± 0.350				
Hérault	C/N > 12	Q > 45	PN% > 2			X		-27.7 ± 0.2	6.1 ± 0.7	13.7 ± 1.2	0.073 ± 0.007	-27.8 ± 0.4	4.7 ± 0.6	8.2 ± 1.5	0.124 ± 0.019
Rhône	C/N > 12	POC% < 1.25	C/N < 6.68 and $\delta^{15}\text{N}$ > 3.92			X		-26.4 ± 1.3	5.2 ± 1.0	17.0 ± 3.2	0.061 ± 0.012	-25.9 ± 0.4	3.1 ± 0.8	8.8 ± 3.1	0.119 ± 0.032

249

250



251 **Table 2** (continued)

River	Phytoplankton				WWTP's POM			
	$\delta^{13}\text{C}$ + equations	$\delta^{15}\text{N}$ + equations	C/N	N/C + equations	$\delta^{13}\text{C}$	$\delta^{15}\text{N}$	C/N	N/C
Seine	-32.8 ± 1.1	8.4 ± 1.7	7.4 ± 0.7	0.136 ± 0.012				
Orne	-31.4 ± 0.8	4.3 ± 0.8	6.6 ± 1.3	0.141 ± 0.010				
Rance	[-31.4;-25;6] ± 1.7	$5.7 \times 10^{-4} \times [\text{chla} + \text{phaeo}] - 0.04 \times [\text{chla} + \text{phaeo}] - 30.6$	[4.7;11.4] ± 0.7	$-0.28 \times [\text{NO}_3] + 12.7$	6.2 ± 0.4	0.161 ± 0.010		
Elorn	-27.4 ± 0.3	6.9 ± 0.5	10.0 ± 0.9	0.101 ± 0.007				
Aulne	-28.1 ± 0.2	8.6 ± 0.2	8.2 ± 0.2	0.122 ± 0.003				
Loire	[-30.6;-25.0] ± 0.9	$5 \times 10^{-4} \times [\text{chla} + \text{phaeo}] - 0.02 [\text{chla} + \text{phaeo}] - 0.39 [\text{chla} / \text{phaeo}] - 27.9$	[3.0;10.4] ± 1.2	$4.2 \times 10^{-4} [\text{chla}] - 0.08 [\text{chla}] + 8.2$	7.2 ± 0.6	0.140 ± 0.011		
Sèvre Niortaise	[-35.7;-29.2] ± 1.0	$-258 \times \exp([\text{chla} + \text{phaeo}] / 16055) - 0.15 \times [\text{temp}] + 229$			[0.106;0.145] ± 0.006	$2.9 \times 10^{-3} \times [\text{chla} + \text{phaeo}] + 0.1$		
Charente	-30.8 ± 0.03	7.5 ± 1.6	6.6 ± 0.3	0.152 ± 0.006				
Seudre	-33.3 ± 0.1							
Porge	-33.6 ± 0.4			0.128 ± 0.008				
Cirès / Renet / Milieu / Lanton / Tagon	-34.9 ± 0.4			0.133 ± 0.006				
Leyre	-30.1 ± 0.3			0.140 ± 0.016				
Landes	-29.9 ± 0.3			0.112 ± 0.010				
Adour	-28.2 ± 0.6			0.111 ± 0.010				
Têt	[-29.7;-27.8] ± 0.6	$-5.2 \times 10^{-3} [\text{temp}]^2 + 0.08 \times [\text{temp}] - 27.5$	[5.3;13.3] ± 1.8	$5.53 \times [\text{temp}] - 5.5$	5.6 ± 0.7	0.181 ± 0.021	-26.3 ± 0.1	-0.7 ± 0.1
Aude	[-32.6;-27.8] ± 0.6	$-0.21 \times [\text{temp}] - 26.5$	[5.2;10.6] ± 1.6	$-1.13 \times \delta^{13}\text{C} - 26.2$	5.0 ± 0.8	0.205 ± 0.033	6.3 ± 0.3	0.160 ± 0.017
Orb	[-30.7;-23.4] ± 0.6	$-0.19 \times [\text{temp}] - 26.0$	[4.9;8.4] ± 0.6	$8.44 - (3.63 \times (\text{conduc} - 505)) / (\text{conduc} - 111)$	4.8 ± 0.9	0.213 ± 0.039	-27.1 ± 0.4	1.9 ± 1.9
Hérault	[-31.5;-27.5] ± 1.0	$-0.19 \times [\text{temp}] - 26.0$	[6.3;10.9] ± 1.3	$3.6 \times 10^{-2} \times [\text{temp}] - 1.15 \times [\text{temp}] + 14.6$	5.0 ± 0.7	0.203 ± 0.031	3.7 ± 3.7	0.270 ± 0.270
Rhône	-27.8 ± 1.2	5.6 ± 0.8	5.5 ± 0.8	0.180 ± 0.030				

252

## 253 2.4. Quantification of POM composition

254 POM composition was quantified using a Bayesian mixing model ('*simmr*' R package version  
 255 0.4.5, Govan and Parnell, 2023) which solves the equations system based on bulk and source  
 256 POM elemental and isotopic signatures. Mixing models were computed for each sampling date  
 257 of each river (Tab. 1), using carbon ( $\delta^{13}\text{C}$  and N/C ratio, Eq. 4, 7, 8), nitrogen ( $\delta^{15}\text{N}$  and C/N  
 258 ratio, Eq. 5, 6, 8), and/or a combination of three ( $\delta^{13}\text{C}$ ,  $\delta^{15}\text{N}$  and N/C ratio, Eq. 4, 5, 7, 8) tracers.  
 259 From the three mixing models performed for each sampling date and river (carbon, nitrogen or  
 260 mixed), one model was selected as the best estimation of bulk POM data. It should be noted  
 261 that N/C and C/N ratios give information on the mixing of C and N, respectively (Perdue and  
 262 Koprivnjak, 2007). We used at least the same number of equations as unknowns (sources) to  
 263 avoid running underdetermined models that result in large uncertainty in model outputs (Phillips  
 264 et al., 2014). Equations of the models were:



$$265 \quad \delta^{13}\text{C}_{\text{mixture}} = x_1 \delta^{13}\text{C}_{\text{source 1}} + x_2 \delta^{13}\text{C}_{\text{source 2}} + x_3 \delta^{13}\text{C}_{\text{source 3}} + x_4 \delta^{13}\text{C}_{\text{source 4}} \quad (\text{Eq. 4})$$

$$266 \quad \delta^{15}\text{N}_{\text{mixture}} = x_1 \delta^{15}\text{N}_{\text{source 1}} + x_2 \delta^{15}\text{N}_{\text{source 2}} + x_3 \delta^{15}\text{N}_{\text{source 3}} + x_4 \delta^{15}\text{N}_{\text{source 4}} \quad (\text{Eq. 5})$$

$$267 \quad \text{C/N}_{\text{mixture}} = x_1 \text{C/N}_{\text{source 1}} + x_2 \text{C/N}_{\text{source 2}} + x_3 \text{C/N}_{\text{source 3}} + x_4 \text{C/N}_{\text{source 4}} \quad (\text{Eq. 6})$$

$$268 \quad \text{N/C}_{\text{mixture}} = x_1 \text{N/C}_{\text{source 1}} + x_2 \text{N/C}_{\text{source 2}} + x_3 \text{N/C}_{\text{source 3}} + x_4 \text{N/C}_{\text{source 4}} \quad (\text{Eq. 7})$$

$$269 \quad x_1 + x_2 + x_3 + x_4 = 1 \quad (\text{Eq. 8})$$

270 As there was no *a priori* knowledge of sources contributions to the POM mixture, the models  
271 were set with an uninformative prior (1, 1, 1, 1) following a Dirichlet distribution (all sources  
272 have an equal probability to contribute to the mix; Phillips et al., 2014). Model runs were set  
273 following the recommendations of Phillips et al. (2014). Models outputs were evaluated with  
274 Gelman-Rubin diagnostic (verification of chain convergence) and predictive distributions to  
275 ensure the good fit of the models to the observed data. Models outputs are given as medians.  
276 Absolute uncertainties for the models varied from 1 to 18 % (range of average for each river)  
277 with an overall average of 8 % (all models).

## 278 **2.5. Forcings at local and multi-systems scales**

279 Environmental forcings driving POM composition were determined using redundancy analysis  
280 (RDA; ‘dudi.pca’ and ‘pcaiv’ functions; R package {ade4} version 1.7-19). RDA summarizes  
281 multiple linear regressions between the response variable (POM composition: mixing model  
282 outputs) and a set of explanatory variables (environmental forcings) to assess causality links  
283 (Legendre et al., 2011). RDAs were performed at single-river and multi-river scales. Regarding  
284 the multi-rivers scale, the annual mean POM composition of each river was used to determine  
285 the drivers of spatial (i.e., between-rivers) variations of POM composition.

286 The proxies of the environmental forcings were chosen to directly or indirectly reflect processes  
287 that occur in the river and the adjacent ecosystems (e.g., primary production, soil leaching or  
288 WWTP’s discharge) influencing POM source inputs and isotopic values. To homogenize the  
289 data sets for running the single-river RDAs, the same combination of twelve proxies for  
290 environmental forcings was used for each river: SPM, chlorophyll *a*, phaeopigments,  
291 temperature, daily river flow, pH, ammonium, nitrates, phosphates, irradiance, zonal and  
292 meridional wind. For the multi-river RDA, environmental proxies were selected to reflect  
293 processes occurring at large spatial scales and in the river basin. Hence, a new combination of  
294 sixteen proxies was used: river flow, conductivity, air temperature, precipitations, zonal and  
295 meridional wind, artificial, agricultural, forest and natural and wetlands surface areas, net soil  
296 erosion, organic carbon content in the soil, river length, basin surface area, latitude, longitude.  
297 From this initial list of proxies, some were removed to limit the auto-correlation (use of the  
298 Variance Inflation Factor, Borcard et al., 2011) and to improve the adjusted R<sup>2</sup> of each RDA  
299 analysis.



## 300        **2.6. Typology of systems**

301 Rivers were classified based on POM composition and its temporal dynamics by performing a  
302 regionalization analysis as in Liénart et al. (2018) (Fig. A1). This method based on multivariate  
303 cluster analysis allows to consider the temporal (seasonal) variations specific to each river in  
304 addition to the spatial (between-rivers) component. The regionalization analysis was based on  
305 POM composition data (i.e., proportions of sources) computed for each river and each month.  
306 When more than twelve months were available (bi-monthly sampling or more years), a standard  
307 year of twelve months was chosen (averaged by month if fortnight dates). (Souissi et al., 2000)

308 A contingency matrix (rivers, sources, months) was created from monthly values of source  
309 contributions (i.e., mixing model outputs). For each month, a dendrogram was performed and  
310 ten cut-off levels were considered. Then, for each cut-off level, similarities between stations  
311 were identified within the twelve-monthly dendrograms. Ultimately, global similarities  
312 between rivers were computed using a fuzzy cluster that returns probabilities of membership of  
313 each river to each cluster type. The best number of river types, i.e., river typology, was  
314 determined considering the best Dunn coefficient (Dunn, 1974) and Silhouette score  
315 (Rousseeuw, 1987).

## 316        **3. Results**

317 Hereafter, four rivers were selected and considered as representative of each type of studied  
318 river (see section 3.4). Thus, most of the results are illustrated using these four rivers. Graphs  
319 of all the other rivers are reported in the supplementary material.

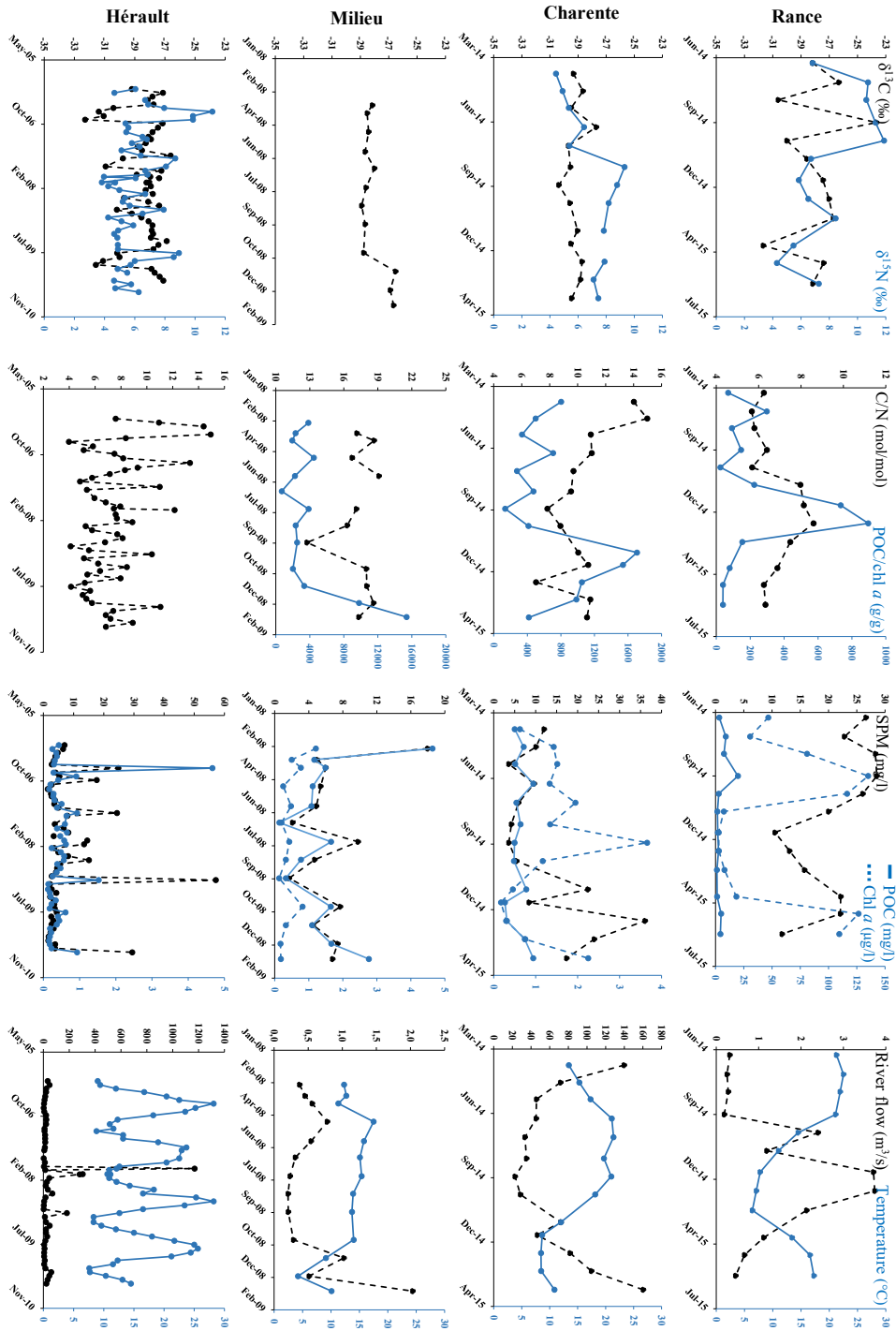
### 320        **3.1. Contrasted seasonalities in river characteristics**

321 As stated in section 2.1, the 23 studied rivers encompassed large gradients of environmental  
322 characteristics, as illustrated by the lowest and highest annual means of river flow (0.3 and 1572  
323 m<sup>3</sup>/s; Lanton and Rhône Rivers), water temperature (12.3 to 17.1 °C; Cirès and Têt Rivers),  
324 SPM (2.7 and 40.9 mg/l; Cirès and Rhône River), POC (0.3 and 5.1 mg/l; Hérault and Loire  
325 Rivers) and chlorophyll *a* (0.4 to 57.1 µg/l; Cirès and Rance Rivers) concentrations as well as  
326 POC/chl *a* (199 and 6444 g/g; Loire and Leyre Rivers) and C/N (5.9 and 20.3 mol/mol; Têt and  
327 Lanton Rivers) ratios; this was less contrasted among rivers for δ<sup>13</sup>C (-30.2 and -26.2 ‰; Sèvre  
328 and Têt Rivers) and especially δ<sup>15</sup>N (4.0 and 8.0 ‰; Leyre and Rance Rivers) (Fig. 2, A2).

329 As generally observed in rivers from mid-latitude, studied rivers exhibited clear seasonal  
330 patterns in water temperature with lower and higher values in winter and summer, respectively.  
331 However, such clear seasonal patterns were not always recorded for all the parameters, as there  
332 were contrasted patterns of seasonal variability among rivers. Indeed, the seasonal variability  
333 of river flow was quite smooth (e.g., the Rance and Charente Rivers) with a higher flow in  
334 winter/spring and lower flow in summer/fall for some rivers, whereas it was highly pulsed for  
335 some others with constant low levels marked by short and strong floods (e.g., 53m<sup>3</sup>/s in mean



336 but 1169m<sup>3</sup>/s in flood time for the Hérault River) (Fig. 2). Overall, one can distinguish rivers  
337 that are characterized by high concentrations of chlorophyll *a* and clear seasonal patterns of  
338 most parameters (e.g., 53 µg/l of chlorophyll *a* in mean ranging from 3 to 135 µg/l in the Rance  
339 River) from rivers characterized by low concentrations of chlorophyll *a*, high POC/chl *a* and  
340 low seasonal variability for most of the parameters (e.g., 1.1 µg/l of chlorophyll *a* in mean  
341 ranging from 0.7 to 1.7 µg/l in the Milieu River) and from rivers that are characterized by high  
342 seasonal variability of most parameters but without a clear seasonal pattern (e.g., Hérault  
343 River). Other rivers exhibited intermediate behavior (e.g., Charente River) (Fig. 2, A2).  
344 Usually, Rance-like rivers exhibited high concentrations of chlorophyll *a* in spring/summer  
345 associated with POC/chl *a* ratio lower than 200 g/g, C/N ratio lower than 8 mol/mol and low  
346 δ<sup>13</sup>C (down to -31 ‰ or -33 ‰; e.g., Seine River, Fig. A2). In contrast, Milieu-like rivers  
347 exhibited high POC/chl *a* (> ~ 700 g/g) and C/N ratio (> 15 mol/mol) and quite constant δ<sup>13</sup>C  
348 (~-29 – -28 ‰) all year round (e.g., Cirès and Renet Rivers). These rivers are tributaries of the  
349 Arcachon Lagoon. Hérault-like rivers flowing into the Mediterranean Sea exhibited highly and  
350 suddenly variable C/N ratios (4 – 17 mol/mol), δ<sup>13</sup>C (~-33 – -26 ‰) and δ<sup>15</sup>N (~2 – 12 ‰) (e.g.,  
351 Aude and Orb Rivers; Fig. A2).







353 Figure 2 Temporal variations of matter characteristics for representative rivers along the studied  
354 periods for  $\delta^{13}\text{C}$  (left axis; black dotted line) and  $\delta^{15}\text{N}$  (right axis; blue line) (first column); C/N  
355 (left axis; black dotted line) and POC/chl *a* (right axis; blue line) ratios (second column);  
356 SPM (left axis; black dotted line), POC (right axis; blue line) and chl *a* (right axis; blue dotted  
357 line) concentrations (third column) and river flow (left axis; black dotted line) and temperature  
358 (right axis; blue line) (fourth column).

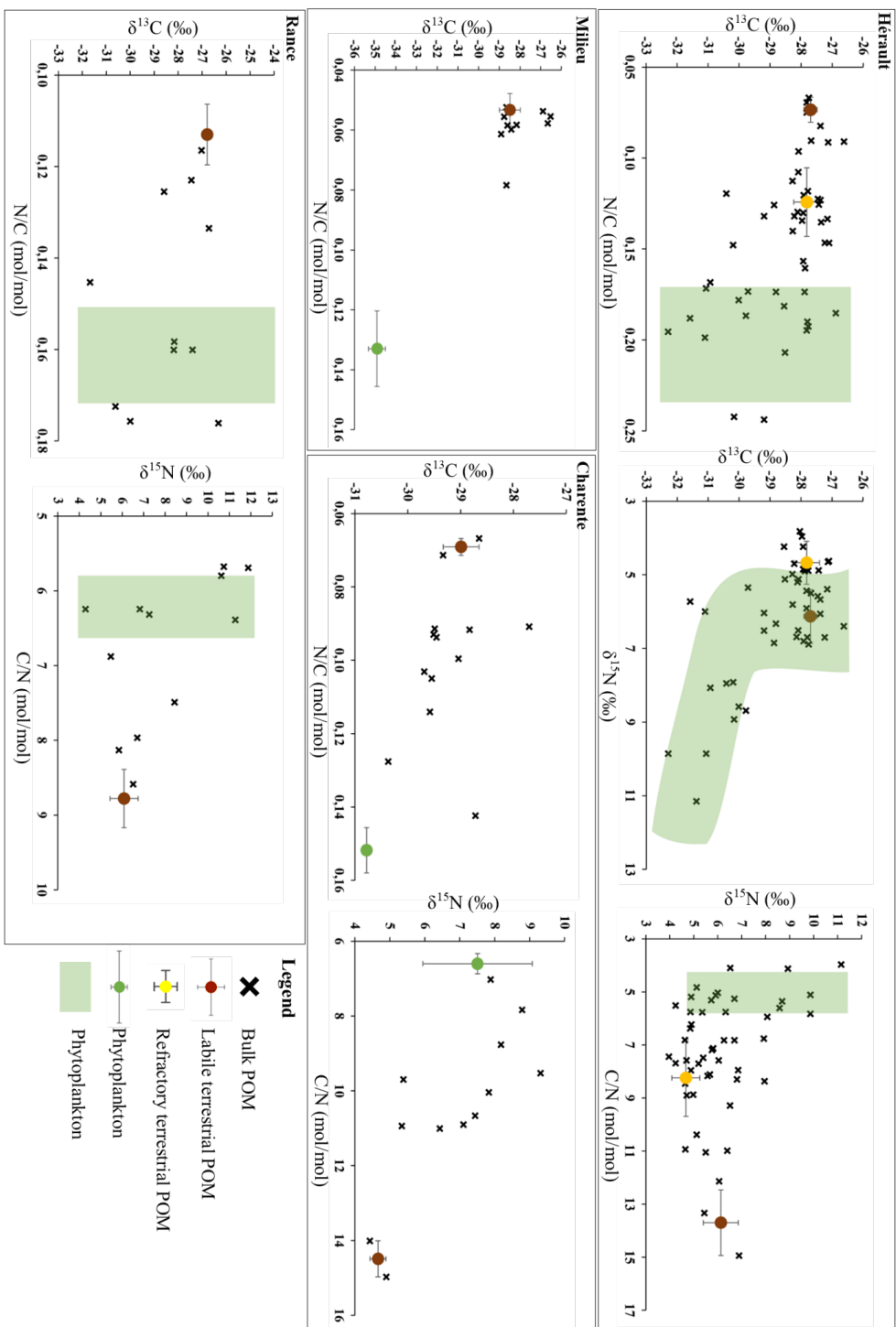
### 359 **3.2. Elemental and isotopic signatures of POM sources**

360 Elemental and isotopic signatures of phytoplankton were estimated for each of the twenty-three  
361 rivers (Tab. 2, Fig. 3 and A3). Most of them (all of them for the C/N ratio) were found constant  
362 over time. Their annual mean values varied between -34.9 ‰ (some tributaries of the Arcachon  
363 Lagoon) and -27.4 ‰ (Elorn River) for  $\delta^{13}\text{C}$ , between 4.3 ‰ (Elorn River) and 8.6 ‰ (Aulne  
364 River) for  $\delta^{15}\text{N}$  and between 4.8 mol/mol (Orb River) and 10.0 mol/mol (Elorn River) for the  
365 C/N ratio. Some of them varied over time along with pigment concentration and ratio or with  
366 temperature for  $\delta^{13}\text{C}$ , and with pigment concentration, nitrate concentration, temperature,  $\delta^{13}\text{C}$   
367 or conductivity for  $\delta^{15}\text{N}$  (Tab. 2). The range of temporal variability was usually 4-6 ‰ for  $\delta^{13}\text{C}$   
368 and  $\delta^{15}\text{N}$ . Overall, phytoplankton signatures are comprised between -35.6 and -23.8 ‰ for the  
369  $\delta^{13}\text{C}$  and between 3.0 and 13.2 ‰ for the  $\delta^{15}\text{N}$ .

370 All other signatures were found constant over time (Tab. 2 and A2, Fig. 3 and A3) but may  
371 differ between rivers. Signatures mean annual values of labile terrestrial POM were comprised  
372 between -29.1 and -26.0 ‰ for the  $\delta^{13}\text{C}$ , between 3.7 and 6.6 ‰ for the  $\delta^{15}\text{N}$  and between 8.8  
373 and 17.0 mol/mol for the C/N ratio. Signatures mean annual values of refractory terrestrial POM  
374 were comprised between -28.0 and -25.9 ‰ for the  $\delta^{13}\text{C}$ , between 3.1 and 6.7 ‰ for the  $\delta^{15}\text{N}$   
375 and between 5.8 and 8.8 mol/mol for the C/N ratio. Signatures mean annual values of sewage  
376 POM were -27.1 and -26.3 ‰ for  $\delta^{13}\text{C}$ , 1.9 and -0.7 ‰ for  $\delta^{15}\text{N}$  and 3.7 and 6.3 mol/mol for  
377 C/N ratio for Orb and Têt Rivers, respectively.



378



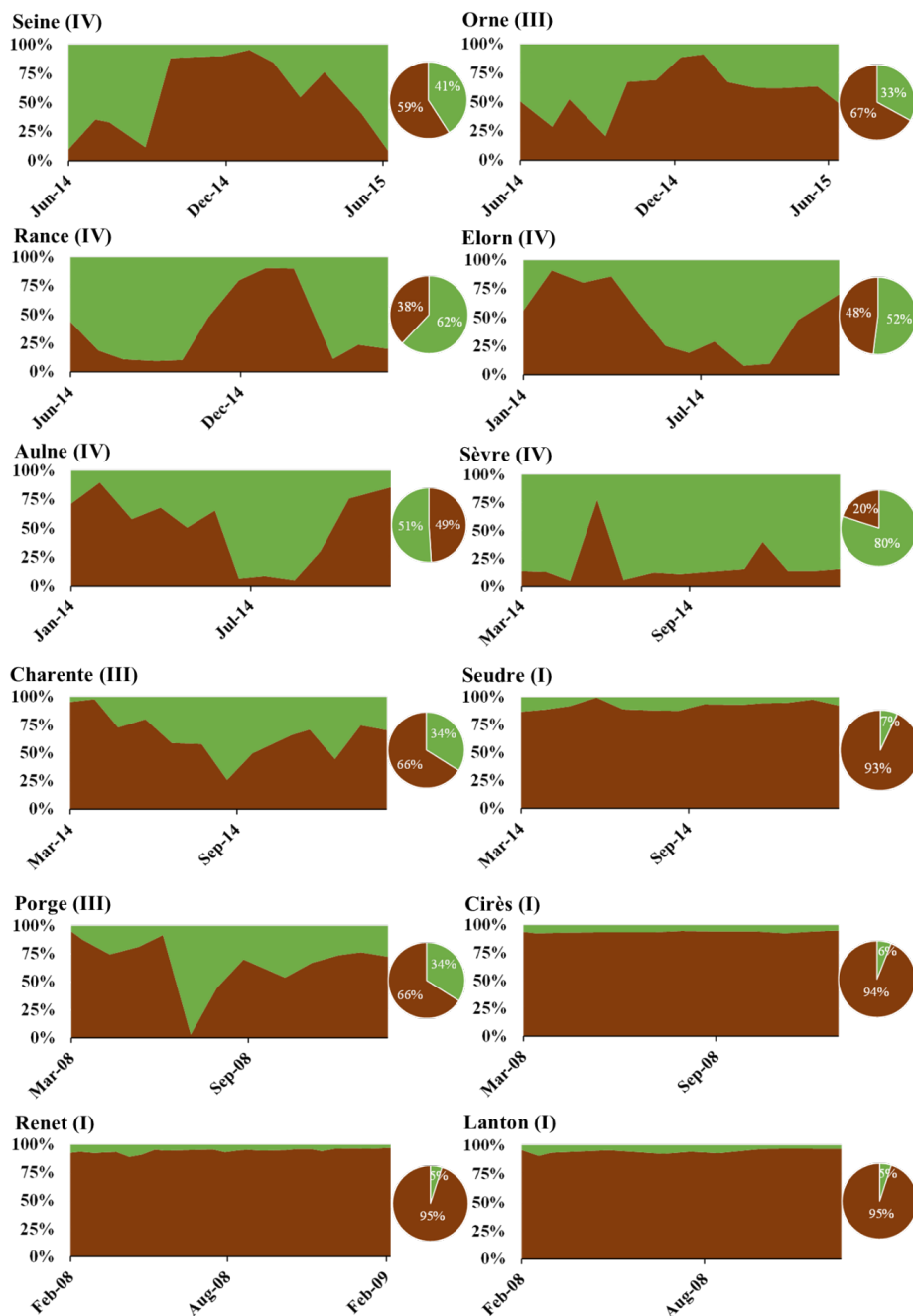


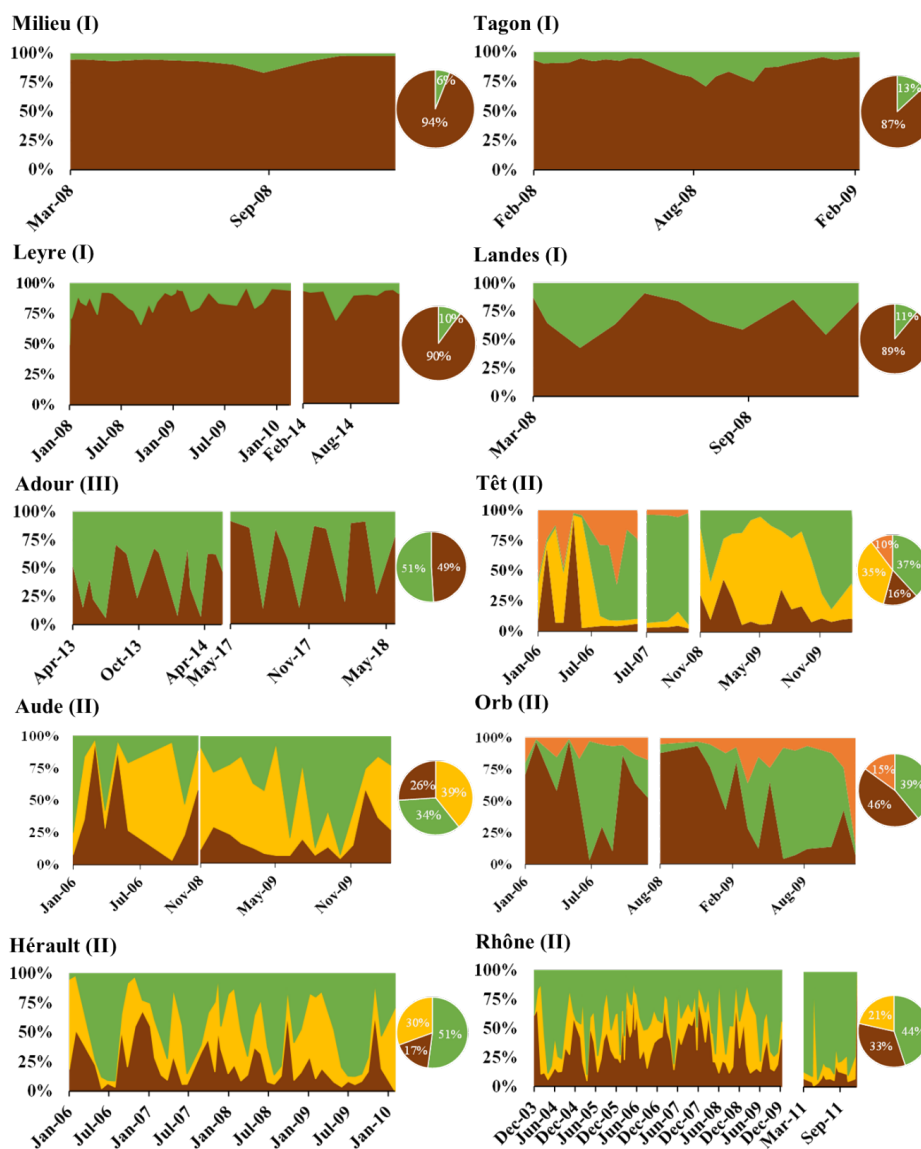
379 Figure 3  $\delta^{13}\text{C}$ ,  $\delta^{15}\text{N}$ , N/C or C/N values of bulk POM (black crosses) and sources. The latter are  
380 presented as closed circles (average) and bars (standard deviation) when the signatures were  
381 constant over time and by colored area when at least one of the proxies was variable over time  
382 (see Table 2). This colored area corresponds to the dispersion of the values including their  
383 uncertainties.

### 384 **3.3. Dynamics of particulate organic matter composition**

385 Particulate organic matter composition resulting from mixing models outputs is presented  
386 hereafter, for each river, as the relative contribution of each source to the POM pool (Fig. 4).  
387 Among rivers whose POM is composed of only two sources (terrestrial POM and  
388 phytoplankton), one can distinguish rivers with terrestrial-dominated POM (e.g., Milieu River:  
389 terrestrial POM accounted for  $94 \pm 3$  % of the mixture) to rivers of intermediate POM  
390 composition (e.g., Charente and Rance Rivers where phytoplankton accounted for  $34 \pm 10$  %  
391 and  $62 \pm 10$  % of the mixture, respectively). All these rivers flow in the English Channel and  
392 the Atlantic Ocean. The rivers whose POM is composed of three or four sources flow in the  
393 Mediterranean Sea. In these rivers, terrestrial POM is present as refractory and labile materials.  
394 The contribution of labile terrestrial POM ranged between  $16 \pm 15$  % (Têt River) and  $46 \pm 21$   
395 % (Orb River), and of refractory terrestrial POM between  $21 \pm 9$  % (Rhône River) and  $39 \pm 15$   
396 % (Aude River). The contribution of phytoplankton ranged between  $34 \pm 15$  % (Aude River)  
397 and  $51 \pm 30$  % (Hérault River) for the Mediterranean rivers. The fourth source of POM was  
398 WWTP's POM. It was identified as a source in the Orb and Têt Rivers and accounted for  $15 \pm$   
399  $6$  % and  $10 \pm 7$  % in these two rivers respectively. Regarding temporal variations of POM  
400 composition, some rivers exhibited clear seasonal patterns whereas others revealed a  
401 homogeneous composition over the annual cycle (Fig. 4). The rivers where POM was highly  
402 dominated by terrestrial POM (Seudre, Cirès, Renet, Lanton, Milieu, Tagon, Leyre Rivers)  
403 showed almost no seasonal variability. In contrast, some rivers like the Rance, the Elorn or the  
404 Aulne River showed a clear seasonal pattern with the dominance of terrestrial material in winter  
405 and phytoplankton in summer. At last, other rivers exhibited less clear (e.g., Landes, Porge,  
406 Charente Rivers) or even no clear seasonal pattern but a quite stochastic variability over the  
407 annual cycle (e.g., Sèvre, Adour, Aude, Orb).

408 It should be noted that the above is valid for carbon and mixed as well as nitrogen models (cf.  
409 Tab. 2; Fig. 4 and A4).





411

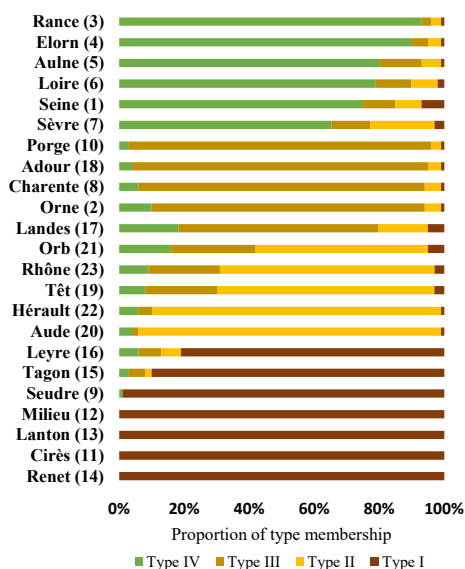
412 Figure 4 Temporal dynamic (rectangle graphs) and (inter-)annual mean (pie charts) of POC  
413 source proportions. Sources are phytoplankton (green), labile terrestrial material (brown),  
414 refractory terrestrial material (yellow) and anthropogenic POM (orange).

415



### 416 3.4. Typology of rivers

417 Four types of rivers were determined by the regionalization analysis based on river POM  
418 composition and its temporal dynamics (Fig. 5). The seven rivers (Renet, Cirès, Lanton, Milieu,  
419 Seudre, Tagon and Leyre River) mainly belonging to Type I are characterized by terrestrial-  
420 dominated POM and no/low seasonality. Six of them are small streams/ivers flowing to the  
421 Arcachon Lagoon. The five rivers (Aude, Hérault, Têt, Rhône and Orb River) mainly belonging  
422 to Type II are characterized by the co-occurrence of labile and refractory terrestrial POM and  
423 large temporal variability but, except for the Hérault River, without a clear seasonal pattern.  
424 They all flow to the Mediterranean Sea. The five rivers (Porge, Adour, Charente, Orne and  
425 Landes River) mainly belonging to Type III are composed of phytoplankton and terrestrial  
426 POM, and exhibit moderate seasonality. Type III is clearly an intermediary between Type I and  
427 Type IV. These five rivers flow to the Atlantic Ocean or the English Channel. Among the seven  
428 rivers flowing to the Arcachon Lagoon, the two that mainly belong to Type III are man-  
429 managed streams and flow through lakes, contrary to the six other ones, which mainly belong  
430 to Type I and are natural streams that do not flow through lakes. Finally, the six rivers (Rance,  
431 Elorn, Aulne, Loire, Seine and Sèvre River) mainly belonging to Type IV are composed of  
432 phytoplankton and terrestrial POM, and exhibit high seasonality. These six rivers flow to the  
433 Atlantic Ocean or the English Channel.



434

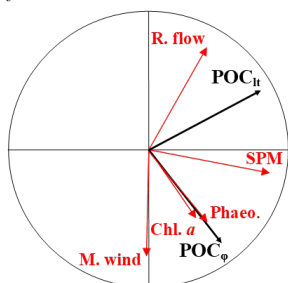
435 Figure 5 Typology of rivers following a hierarchical cluster analysis on POM source  
436 proportions. The percentages of membership for each type attributed to each river are shown.

### 437 3.5. Environmental forcings driving POM composition

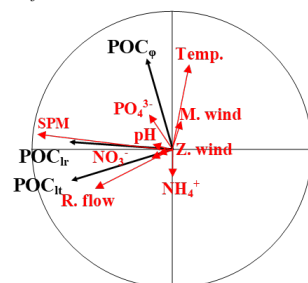


438 One redundancy analysis was performed for each river to relate environmental parameters,  
 439 considered as proxies of drivers, to the POM composition, i.e., to assess the drivers of the  
 440 temporal variability of POM composition for each river (Fig. 6 and A5). It should be kept in  
 441 mind that the POC or PN concentration of each source was used for these analyses and not the  
 442 relative proportion of the sources. In type-I rivers, i.e., rivers characterized by terrestrial-  
 443 dominated POM and no/low seasonality, terrestrial POM is usually linked to river flow and/or  
 444 SPM concentration (e.g., Milieu River on Fig. 6, Leyre and Tagon Rivers in Fig. A5). However,  
 445 this feature is not always clear since the POM of these rivers is always dominated by terrestrial  
 446 material, almost whatever the environmental conditions are. In type-II rivers, i.e., rivers  
 447 characterized by the co-occurrence of labile and refractory terrestrial POM and large temporal  
 448 variability, phytoplankton POM is usually positively linked to temperature and negatively  
 449 linked to river flow, whereas labile and refractory terrestrial POM is positively linked to SPM  
 450 and/or river flow. Interestingly, labile terrestrial POM is usually better linked to river flow and  
 451 refractory terrestrial POM to SPM (e.g., Hérault River in Fig. 6 and Rhône River in Fig. A5).  
 452 In the Têt River, anthropogenic POM was linked to nitrate concentration (Fig. A5). In rivers  
 453 characterized by phytoplankton and terrestrial-POM composition with moderate (Type III) or  
 454 high (Type IV) seasonality, terrestrial POM was almost always positively linked to river flow  
 455 and/or SPM concentration while phytoplankton was usually linked with chl *a* concentration  
 456 (e.g., Charente and Rance River on Fig. 6, Landes and seine River on Fig. A5).

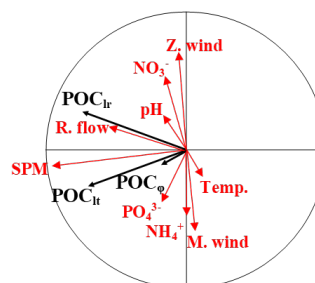
**Milieu (I)**  
*Adj. R<sup>2</sup> 0.76*



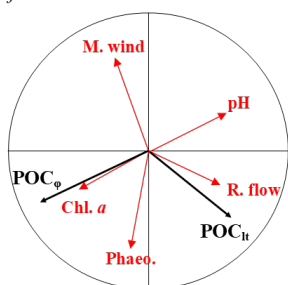
**Hérault (axis 1-2) (II)**  
*Adj. R<sup>2</sup> 0.49*



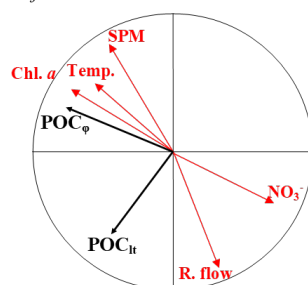
**Hérault (axis 1-3) (II)**



**Charente C (III)**  
*Adj. R<sup>2</sup> 0.50*



**Rance C (IV)**  
*Adj. R<sup>2</sup> 0.35*

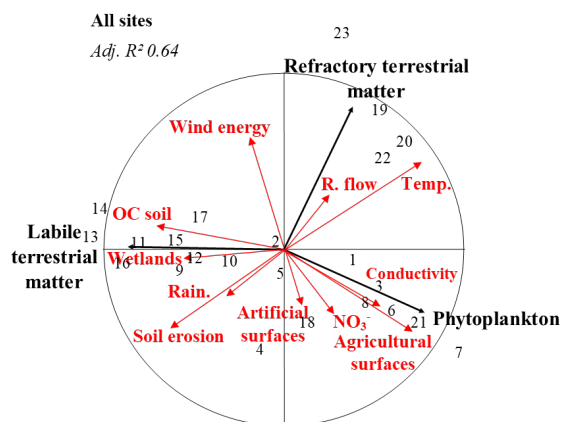


457



458 Figure 6 Redundancy analyses (correlation circles) of rivers standing for each type of river.  
459 Black arrows represent explained variables (concentration of POC sources) and red arrows  
460 represent explaining variables (environmental variables). River types are recalled (Roman  
461 numerals).  $POC_{lt}$  = Labile terrestrial POC;  $POC_{rt}$  = Refractory terrestrial POC;  $POC_{\phi}$  =  
462 Phytoplankton POC; Chl a = chlorophyll a; Phaeo. = phaeopigments; M. wind = meridional  
463 wind; Z. wind = zonal wind; R. flow = river flow; Temp. = temperature; Irrad. = Irradiance;  
464  $NH_4^+$  = ammonium;  $NO_3^-$  = nitrate;  $PO_4^{3-}$  = phosphates ; Adj.  $R^2$  = adjusted  $R^2$ .

465 At last, another RDA was performed gathering all rivers to relate environmental parameters to  
466 the mean annual POM composition at the multi-rivers scale (Fig. 7). As anthropogenic POM  
467 was only detected in two rivers (Orb, Têt), it was not included in the multi-rivers analysis to  
468 avoid analysis bias. At this scale, phytoplankton is strongly positively linked to agricultural  
469 surfaces, labile terrestrial material to soil erosion rate and soil organic carbon and refractory  
470 terrestrial material to river flow and water temperature.



471

472 Figure 7 Multi-rivers redundancy analysis. Black arrows represent explained variables (relative  
473 proportions), red arrows represent explaining variables (environmental variables) and numbers  
474 are river identifiers (cf. Fig.1). R. flow = river flow; OC soil = percentages of organic carbon  
475 in soil; Soil erosion = soil erosion rate; Rain. = precipitations;  $NO_3^-$  = nitrate concentration ;  
476 Adj.  $R^2$  = adjusted  $R^2$ .

## 477 4. Discussion

### 478 4.1. Bulk data and source signatures in temperate rivers

479 Over the 23 studied rivers,  $\delta^{13}C$ ,  $\delta^{15}N$  and C/N ratios of bulk POM ranged between -35.2 and -  
480 24.5 ‰, -0.3 and 12.6 ‰, and 3 and 23.4 mol/mol, respectively. This corresponds to usual  
481 values recorded for riverine POM over temperate systems, except for the lowest C/N ratios  
482 (Ferchiche et al., 2024; Kendall et al., 2001; Ogrinc et al., 2008).





483 In the present study, isotopic and elemental signatures of terrestrial POM and phytoplankton  
484 were determined from subsets of the bulk data sets following the approaches of Savoye et al.  
485 (2012), Liénart et al. (2017) and Ferchiche et al. (2025, 2024). It has the double advantage of  
486 1) taking into account the reworking of terrestrial POM within the river and thus discriminating  
487 labile from refractory terrestrial POM, and 2) taking into account the variability of  
488 phytoplankton signature over time, due to differences in growth conditions (see below). Labile  
489 terrestrial POM mainly appears during high river flow (Fig. 6 and A5; Savoye et al., 2012) and  
490 is usually composed of riparian litter (e.g., Veyssy et al., 1998). In the studied rivers,  $\delta^{13}\text{C}$ ,  $\delta^{15}\text{N}$   
491 and C/N ratio of labile terrestrial POM ranged between  $-28.9 \pm 0.8 \text{ ‰}$  and  $-26 \pm 0.9 \text{ ‰}$ ,  $3.7 \pm$   
492  $0.6 \text{ ‰}$  and  $6.6 \pm 0.9 \text{ ‰}$ , and  $8.8 \pm 0.4$  and  $17 \pm 3.2 \text{ mol/mol}$ , respectively. These values are very  
493 similar to values found in other temperate systems like the Gironde Estuary ( $\delta^{13}\text{C} = -28.7 \pm 0.9$   
494  $\text{‰}$ ; Savoye et al., 2012), the Sava River ( $\delta^{13}\text{C} = -28 \pm 5 \text{ ‰}$ ;  $\delta^{15}\text{N} = 5 \pm 2 \text{ ‰}$ ; C/N =  $33 \pm 15$   
495  $\text{mol/mol}$ ; Ogrinc et al., 2008) or Taiwanese rivers ( $\delta^{13}\text{C} = -26.6 \pm 1.8 \text{ ‰}$ ; C/N =  $31.1 \pm 23.4$   
496  $\text{mol/mol}$ ; Hilton et al., 2010) and very similar to direct measurement of C3 plants ( $\delta^{13}\text{C} = -28.1$   
497  $\pm 2.5 \text{ ‰}$ ; O'Leary, 1981 and references therein;  $\delta^{13}\text{C} = -28 \pm 1.3 \text{ ‰}$ ;  $\delta^{15}\text{N} = 0.8 \pm 2.9 \text{ ‰}$ ; C/N  
498 =  $39.6 \pm 25.7 \text{ mol/mol}$ ; Dubois et al., 2012;  $\delta^{13}\text{C} = -27.9 \pm 0.1 \text{ ‰}$ ; Fernandez et al., 2003).  
499 Refractory terrestrial POM is terrestrial POM that has undergone large reworking within river  
500 water, river sediment or even estuarine maximum turbidity zone (e.g., Etcheber et al., 2007;  
501 Veyssy et al., 1998). In the studied rivers where it was found,  $\delta^{13}\text{C}$ ,  $\delta^{15}\text{N}$  and C/N ratios of  
502 refractory terrestrial POM ranged between  $-28 \pm 0.7 \text{ ‰}$  and  $-25.9 \pm 0.4 \text{ ‰}$ ,  $3.2 \pm 0.8 \text{ ‰}$  and  $6.7$   
503  $\pm 1.4 \text{ ‰}$ , and  $5.8 \pm 1.4$  and  $8.8 \pm 3.1 \text{ mol/mol}$ , respectively. These values are very similar to  
504 those found in other systems like the Gironde Estuary (France) ( $\delta^{13}\text{C} = -25.2 \pm 0.3 \text{ ‰}$ ;  $\delta^{15}\text{N} =$   
505  $5.5 \pm 0.4 \text{ ‰}$ ; C/N =  $8.5 \pm 0.8 \text{ mol/mol}$ ; Savoye et al., 2012), Taiwanese rivers ( $\delta^{13}\text{C} = -23.6 \pm$   
506  $1.1 \text{ ‰}$ ; C/N =  $6.5 \pm 1.6 \text{ mol/mol}$ ; Hilton et al., 2010) and in the Pearl River (China) ( $\delta^{13}\text{C}$ :  
507 between  $-28.3 \pm 0.8 \text{ ‰}$  and  $-21.7 \pm 0.7 \text{ ‰}$ ; C/N: between  $8.9 \pm 1.1$  and  $17.9 \pm 3.6 \text{ mol/mol}$ ; Yu  
508 et al., 2010).

509 Isotopic signatures of phytoplankton vary depending on biogeochemical conditions and  
510 processes like nutrient availability and utilization, growth rate and limitation (e.g., Fry, 1996;  
511 Liénart et al., 2017; Lowe et al., 2014; Miller et al., 2013; Savoye et al., 2003; Sigman et al.,  
512 2009; Yan et al., 2022) and can be estimated using measured environmental parameters  
513 (Ferchiche et al., 2024, 2025; Liénart et al., 2017; Savoye et al., 2012). For the seven rivers  
514 where phytoplankton isotopic signatures were found variable over time, phytoplankton  $\delta^{13}\text{C}$  or  
515  $\delta^{15}\text{N}$  were correlated to: concentrations and ratio of chlorophyll *a* and phaeopigments, water  
516 temperature, nitrate concentration and/or conductivity (Tab. 2). Chlorophyll *a* and  
517 phaeopigments concentrations are direct proxies of phytoplankton fresh and degraded  
518 biomasses and are related to phytoplankton growth and decay, two processes that increase  
519 phytoplankton  $\delta^{13}\text{C}$  (Golubkov et al., 2020; Michener and Kaufman, 2007 and references



520 therein). Similar processes may explain phytoplankton- $\delta^{15}\text{N}$  increase with chlorophyll *a*  
521 increase. An increase in water temperature accelerates bio-mediated carbon remineralization  
522 processes bringing a lower  $\delta^{13}\text{C}$  value than  $\text{CO}_2$  coming from water-atmosphere equilibration  
523 and rock-leaching  $\text{CO}_2$  (Polsenaere et al., 2013 and references therein). Consequently,  
524 phytoplankton  $\delta^{13}\text{C}$  decreases as phytoplankton uses remineralized  $\text{CO}_2$  and thus as water  
525 temperature increases. Phytoplankton  $\delta^{15}\text{N}$  depends on N-nutrient origin and availability  
526 (Savoye et al., 2003 and references therein). Especially, it increases with nutrient concentration  
527 decrease (Sigman et al., 2009) as reported for the Rance River (Tab. 2). Water conductivity  
528 could be considered as a proxy of water mass and thus of nitrate origin. This may explain the  
529 relationship between phytoplankton  $\delta^{15}\text{N}$  and water conductivity in the Orb River (Tab. 2).

530 In the studied rivers, phytoplankton  $\delta^{13}\text{C}$ ,  $\delta^{15}\text{N}$  and C/N ratio ranged between  $-34.9 \pm 0.4$  and -  
531  $23.8 \pm 0.6$  ‰,  $4.3 \pm 0.8$  and  $13.2 \pm 1.8$  ‰, and  $4.8 \pm 0.9$  and  $10 \pm 0.9$  mol/mol, respectively.  
532 This is similar to values reported for the Loire River, another French river ( $-30.6 \leq \delta^{13}\text{C} \leq -25.0$   
533 ‰;  $3.0 \leq \delta^{15}\text{N} \leq 10.4$  ‰; C/N =  $7.2 \pm 0.6$  mol/mol; Ferchiche et al, 2024) but narrower ranges  
534 can be found in the literature. In the Sava River (Eastern Europe), phytoplankton signature was  
535  $-30.4 \pm 2.1$  ‰,  $5.0 \pm 1.5$  ‰ and  $6.5 \pm 1.5$  mol/mol for  $\delta^{13}\text{C}$ ,  $\delta^{15}\text{N}$  and C/N ratio, respectively  
536 (Ogrinc et al., 2008), similar to that of Indian ( $\delta^{13}\text{C} = -30.6 \pm 1.7$  ‰,  $\delta^{15}\text{N} = 7.0 \pm 2.3$  ‰;  
537 Gawade et al., 2018) and Texan ( $\delta^{13}\text{C} = -31.4$  ‰; Lebreton et al., 2016) rivers. Lower  $\delta^{13}\text{C}$   
538 values ( $\leq -32$  ‰) were also found (Finlay et al., 2010; Hellings et al., 1999; Sato et al., 2006;  
539 Savoye et al., 2012). However, values of elemental and isotopic ratios for riverine  
540 phytoplankton are scarce in the literature. Indeed, it is not easy to estimate phytoplankton  
541 signature since it cannot be separated from other particles. Thus, literature estimates may not  
542 be perfectly representative of the variability of phytoplankton isotopic signatures.

#### 543 **4.2. Watershed characteristic drive on spatial dynamics of POM** 544 **composition**

545 At the annual scale, we observed deep variations between studied rivers concerning the mean  
546 POC proportion of the different sources ( $5 \leq$  phytoplankton  $\leq 80$  %;  $17 \leq$  labile terrestrial POC  
547  $\leq 95$  %;  $0 \leq$  refractory terrestrial POC  $\leq 39$  %). Interestingly, phytoplankton proportion was  
548 highly correlated to the proportion of agriculture surface area (Fig. 7;  $R^2 = 0.59$  or even 0.72  
549 when Seudre River is not included in the statistics) and nitrate concentration (Fig. 7;  $R^2 = 0.41$   
550 when Seudre River is not included in the statistics). Such relationship between agriculture  
551 surface area and phytoplankton is well-known, as agricultural activities increase nutrient input  
552 to river bodies (Khan and Mohammad, 2014), leading to better conditions for phytoplankton  
553 growth (Dodds and Smith, 2016; Minaudo et al., 2015). Interestingly, the proportion of labile  
554 terrestrial matter was strongly linked to soil erosion and soil organic carbon content (Fig. 7)  
555 indicating a strong relationship between terrestrial matter in rivers and soil nature with  
556 undecomposed and fresh detrital matter (McCorkle et al., 2016).



### 557 **4.3. Temporal dynamics of POM composition and river typology**

558 In aquatic systems, phytoplankton likely appears during spring and summer in favorable  
559 conditions, related to low discharge, high-temperature conditions and enough nutrients to  
560 support its growth, while in winter, high turbidity and low-temperature conditions limit its  
561 presence (Turner et al., 2022). Quantitative differences between rivers can be due to differences  
562 in nutrient availability, either because of anthropic mitigation (Minaudo et al., 2015),  
563 competition with other nutrient users (Descy et al., 2012; Minaudo et al., 2016) or sewage inputs  
564 (Codiga et al., 2022) in addition to agricultural inputs (see section 4.2). Terrestrial material  
565 likely appears during winter conditions, related to floods that transport great amounts of  
566 terrestrial material (Dalzell et al., 2007). Such a seasonal dichotomy between phytoplankton  
567 and terrestrial POM was clearly visible for most of the studied rivers (Fig. 4), especially for  
568 type-IV and type-III rivers, but even for some of those highly dominated by the labile terrestrial  
569 POM (e.g., Milieu and Tagon Rivers; Type-I rivers). This was illustrated by the relationships  
570 between phytoplankton POM and chlorophyll *a* concentration and/or temperature (as proxies  
571 of favorable conditions for phytoplankton production) on the one hand, and between labile  
572 terrestrial POM and river flow and/or SPM concentration on the other hand (Fig. 6 and A5).  
573 This dichotomy in POM composition was also reported in other similar studies (e.g., Kelso and  
574 Baker, 2020; Lu et al., 2016). In rivers where refractory terrestrial POM was present in addition  
575 to the labile one (type-II rivers), it was interesting to see that the refractory terrestrial POM was  
576 more related to SPM concentration than river flow and inversely for the labile terrestrial POM.  
577 This indicates that labile and refractory terrestrial POM were preferentially associated with  
578 direct river input and sediment resuspension, respectively. The origin of the refractory terrestrial  
579 POM may be fossil/bedrock/petrogenic OM (e.g., Copard et al., 2022; Hilton et al., 2010; Sun  
580 et al., 2021) brought by river flow (in quantity undetectable in the bulk POM using our tools)  
581 and then accumulated in the sediment, and/or labile terrestrial POM brought by the river flow  
582 and then accumulated and reworked/decayed in the sediment (e.g., Etcheber et al., 2007; Savoye  
583 et al., 2012).

584 Sewage POM was detected in two of the studied rivers but with different associated temporal  
585 dynamics. In the Têt River, because the former WWTP was dysfunctional, a new one replaced  
586 it in late 2007 ([https://www.assainissement.developpement-durable.gouv.fr/pages/data/fiche-  
587 060966136002](https://www.assainissement.developpement-durable.gouv.fr/pages/data/fiche-060966136002), last visit 10/09/24). This explains the shift in sewage POM between the two  
588 studied periods (2006-2007 versus 2008-2010 without anthropogenic POM). In the Orb River,  
589 sewage POM was detected throughout the studied periods. The WWTP is located only a few  
590 kilometers upstream of the sampling site and is large enough (220 000 inhabitant equivalent)  
591 compared to the river flow (annual mean: 23m<sup>3</sup>/s) to make the sewage POM detectable in the  
592 bulk POM using  $\delta^{15}\text{N}$ . Such a result is quite common for urban rivers (e.g., Kelso and Baker,  
593 2020).



#### 594 **4.4. Originality of the study**

595 The originality of the present study firstly lies in its approach. Even if C and N stable isotopes  
596 have been used for decades to investigate POM origins within river waters, the quantification  
597 of POM composition (i.e., the relative proportion of each source composing the POM) using  
598 mixing models, and especially Bayesian mixing models, is not so common. In addition, most  
599 of the previous studies either use literature data for phytoplankton isotopic signature (e.g.,  
600 Zhang et al., 2021) or use lake or autochthonous POM as a proxy of phytoplankton (e.g., Kelso  
601 and Baker, 2020). Also, most of these studies use direct measurements of soil or plants to assess  
602 the isotopic signature of terrestrial POM whereas this material is able to rework within the water  
603 column or the sediment, which changes its elemental and isotopic values (e.g., Savoye et al.,  
604 2012). These approaches do not consider that isotopic signatures of phytoplankton and  
605 terrestrial material may change over time. In the present study, we used the approach developed  
606 by Savoye et al. (2012) in an estuary, Liénart et al. (2017) in coastal systems and Ferchiche et  
607 al. (2025, 2024) in a river to assess the elemental and isotopic signatures from subsets of bulk  
608 POM and when needed, empirical equations. This approach has the great advantage of 1) using  
609 signatures dedicated to the sampling area and 2) taking into account the potential variability of  
610 these signatures over time, i.e., depending on the environmental conditions for phytoplankton  
611 growth and taking into account its decay for phytoplankton and terrestrial POM. Especially, we  
612 were able to discriminate labile from refractory terrestrial POM in some rivers, as Savoye et al.  
613 (2012) in an estuary. Another great originality of the present study lies in the multi-systems  
614 approach: studying 23 rivers in a single study allowed the detection of four types of river  
615 functioning regarding the POM composition and its temporal dynamics. It also highlights the  
616 great influence of land use (agriculture) and characteristics (erosion, organic carbon content)  
617 on the POM composition of rivers. At last, using  $\delta^{13}\text{C}$ ,  $\delta^{15}\text{N}$  and C/N ratio all together allowed  
618 either to perform mixing models with up to four end-members or to study separately POC and  
619 PN composition. It showed that POC and PN display very similar compositions and dynamics  
620 in rivers.

#### 621 **5. Synthesis and perspectives**

622 The present study proposes a comprehensive estimation of POM composition and its spatial  
623 and seasonal variability in temperate rivers. Thanks to the inclusion of twenty-three rivers,  
624 encompassing large gradients of environmental conditions under a temperate climate, a river  
625 typology is proposed based on the POM composition and its temporal dynamics. In type-I  
626 rivers, POM is dominated by labile terrestrial material all year long. This material is mainly  
627 associated with suspended particulate matter. Phytoplankton slightly contributes, especially  
628 during summertime. Type-II rivers are mainly characterized by the presence of both labile and  
629 refractory terrestrial material, in addition to phytoplankton. The temporal variability between  
630 these sources is high but the seasonality is not always pronounced even if phytoplankton and



631 terrestrial POM can dominate the POM composition during summer and winter, respectively.  
632 Nevertheless, labile terrestrial POM is mainly related to river flow and refractory terrestrial  
633 POM to SPM, indicating the sedimentary origin of the latter. In type-III rivers, POM is  
634 composed of phytoplankton and labile terrestrial material. The seasonality of POM composition  
635 is not very pronounced even if the contribution of labile terrestrial POM is deeply related to  
636 river flows. Type III is an intermediary between type I and type IV. In type-IV rivers, POM is  
637 also composed of phytoplankton and labile terrestrial material but the seasonality of POM  
638 composition is very pronounced with a clear balance between high phytoplankton contribution  
639 in summer and high terrestrial contribution in winter. Labile terrestrial POM is deeply related  
640 to river flow. Beyond this typology, the main difference in POM composition between the  
641 studied rivers is that the phytoplankton contribution to the POM composition is related to the  
642 proportion of agricultural surface in the watershed and the contribution of labile terrestrial POM  
643 is related to soil erosion and organic carbon content in the watershed.

644 The originality of this study mainly lies in 1) the approach used to determine the elemental and  
645 isotopic signatures of POM sources, which allowed to discriminate labile from refractory  
646 terrestrial POM and to take into account, when any, the variability of the signatures over time,  
647 and 2) determining a typology of temperate rivers based on the POM composition and its  
648 temporal dynamics.

649 Overall, this study, which focuses on the River-Estuary Interface, brings meaningful  
650 information for the comprehension of C and N cycles along the LOAC and especially the  
651 behavior, dynamics and drivers of POM that leaves the river and enters the estuary.

652 From a methodological perspective, such a study could be strengthened by the use of non-  
653 exchangeable  $\delta^2\text{H}$  as an additional tool to even better distinguish and quantify more sources in  
654 mixing models. This tool has been recently shown to be powerful for such purposes (Ferchiche  
655 et al., 2025). From a fundamental perspective, aggregating more datasets from other temperate  
656 rivers would allow testing the robustness of this typology and probably detecting additional  
657 types, but also datasets from polar and tropical rivers to perform an even more comprehensive  
658 study at a global climate scale. In addition, a similar study dedicated to the estuarine systems  
659 would even increase our comprehensive understanding of the origin and fate of POM along the  
660 Land-Ocean Aquatic Continuum by complementing the present study dedicated to the River-  
661 Estuary Interface and those of Liénart et al. (2017, 2018) dedicated to the coastal systems.

662



663

## *Appendix*

664 **Toward a typology of river functioning: a**  
665 **comprehensive study of POM composition at multi-**  
666 **rivers scale**

667

668 Ferchiche F.<sup>1</sup>, Liénart C.<sup>1</sup>, Charlier K.<sup>1</sup>, Deborde J.<sup>2,3</sup>, Giraud M.<sup>4</sup>, Kerhervé P.<sup>5</sup>, Polsenaere P.<sup>1,3</sup>, Savoye  
669 N.<sup>1\*</sup>

670 <sup>1</sup> Univ. Bordeaux, CNRS, EPHE, Bordeaux INP, UMR 5805 EPOC, F-33600 Pessac, France

671 <sup>2</sup> Univ. Pau & Pays Adour, CNRS, E2S UPPA – MIRA, UMR 5254 IPREM, F-64000 Pau, F-64600 Anglet, France

672 <sup>3</sup> Ifremer, COAST, F-17390 La Tremblade, France

673 <sup>4</sup> MNHN, CRESCO, Station Marine de Dinard, F-35800 Dinard, France

674 <sup>5</sup> Univ. Perpignan, CNRS, UMR 5110 CEFREM, F-66860 Perpignan, France

675

676 \*Corresponding author

677 [nicolas.savoye@u-bordeaux.fr](mailto:nicolas.savoye@u-bordeaux.fr)

678 Station marine - 2 rue du Professeur Jolyet 33120 ARCACHON

679

680

681

682

683

684

685

686

687

688

689

690

691

692 Keywords : River-Estuary Interface; particulate organic matter; isotopes; multi-ecosystems  
693 study



694  
 695 **Table A1** Summary of data availability and origin (X means that the data were available; \* means that the data were retrieved from the Natades  
 696 database; \*\* means that the data were retrieved from the Météo France database). n = number of sampling dates; SPM = Suspended Particulate  
 697 Matter; POC or PN = Particulate Organic Carbon or Nitrogen; Chl *a* = Chlorophyll *a*; Phaeo = Phaeocigments.

River	Dates	Periodicity	Samplings			Parameters																							
			n	Latitude	Longitude	$\delta^{13}\text{C}$	$\delta^{15}\text{N}$	C/N ratio	SPM	POC	PN	Chl <i>a</i>	Phaeo	temperat ure	pH	Cond. enviry	NH <sub>4</sub> <sup>+</sup>	NO <sub>2</sub> <sup>-</sup>	NO <sub>3</sub> <sup>-</sup>	PO <sub>4</sub> <sup>3-</sup>	Flow	Rainfall	tempera ture	Wind direction	Wind intensity	Tradi ance			
Seine	06/2014 to 06/2015	monthly	13	49.306667	1.242500	X	X	X <sup>*</sup>	X	X	X	X	X	X <sup>*</sup>	X <sup>*</sup>	X <sup>*</sup>	X <sup>*</sup>	X <sup>*</sup>	X <sup>*</sup>	X <sup>*</sup>	X	X	X <sup>**</sup>	X <sup>**</sup>	X <sup>**</sup>	X <sup>**</sup>	X <sup>**</sup>	X <sup>**</sup>	X <sup>**</sup>
Orne	06/2014 to 06/2015	monthly	13	49.179722	-0.349167	X	X	X <sup>*</sup>	X	X	X	X	X	X <sup>*</sup>	X <sup>*</sup>	X <sup>*</sup>	X <sup>*</sup>	X <sup>*</sup>	X <sup>*</sup>	X <sup>*</sup>	X	X	X <sup>**</sup>	X <sup>**</sup>	X <sup>**</sup>	X <sup>**</sup>	X <sup>**</sup>	X <sup>**</sup>	X <sup>**</sup>
Rance	06/2014 to 05/2015	monthly	12	48.491667	-2.001389	X	X	X <sup>*</sup>	X	X	X	X	X	X <sup>*</sup>	X <sup>*</sup>	X <sup>*</sup>	X <sup>*</sup>	X <sup>*</sup>	X <sup>*</sup>	X <sup>*</sup>	X	X	X <sup>**</sup>	X <sup>**</sup>	X <sup>**</sup>	X <sup>**</sup>	X <sup>**</sup>	X <sup>**</sup>	X <sup>**</sup>
Eloren	01/2014 to 06/2015	monthly	17	48.450556	-4.248333	X	X	X <sup>*</sup>	X	X	X	X	X	X <sup>*</sup>	X <sup>*</sup>	X <sup>*</sup>	X <sup>*</sup>	X <sup>*</sup>	X <sup>*</sup>	X <sup>*</sup>	X	X	X <sup>**</sup>	X <sup>**</sup>	X <sup>**</sup>	X <sup>**</sup>	X <sup>**</sup>	X <sup>**</sup>	X <sup>**</sup>
Aulne	01/2014 to 06/2015	monthly	17	48.212778	-4.094444	X	X	X <sup>*</sup>	X	X	X	X	X	X <sup>*</sup>	X <sup>*</sup>	X <sup>*</sup>	X <sup>*</sup>	X <sup>*</sup>	X <sup>*</sup>	X <sup>*</sup>	X	X	X <sup>**</sup>	X <sup>**</sup>	X <sup>**</sup>	X <sup>**</sup>	X <sup>**</sup>	X <sup>**</sup>	X <sup>**</sup>
Loire	10/2009 to 07/2012	bi-monthly	67	47.392095	-0.860351	X	X	X <sup>*</sup>	X	X <sup>*</sup>	X	X	X	X	X	X	X	X	X	X	X	X	X <sup>**</sup>	X <sup>**</sup>	X <sup>**</sup>	X <sup>**</sup>	X <sup>**</sup>	X <sup>**</sup>	X <sup>**</sup>
Sèvre nioraise	03/2014 to 03/2015	monthly	13	46.315348	-1.003891	X	X	X <sup>*</sup>	X	X <sup>*</sup>	X	X	X	X <sup>*</sup>	X <sup>*</sup>	X <sup>*</sup>	X <sup>*</sup>	X <sup>*</sup>	X <sup>*</sup>	X <sup>*</sup>	X	X	X <sup>**</sup>	X <sup>**</sup>	X <sup>**</sup>	X <sup>**</sup>	X <sup>**</sup>	X <sup>**</sup>	X <sup>**</sup>
Charente	03/2014 to 03/2015	monthly	13	45.868056	-0.713056	X	X	X <sup>*</sup>	X	X <sup>*</sup>	X	X	X	X <sup>*</sup>	X <sup>*</sup>	X <sup>*</sup>	X <sup>*</sup>	X <sup>*</sup>	X <sup>*</sup>	X <sup>*</sup>	X	X	X <sup>**</sup>	X <sup>**</sup>	X <sup>**</sup>	X <sup>**</sup>	X <sup>**</sup>	X <sup>**</sup>	X <sup>**</sup>
Scudre	03/2014 to 09/2015	monthly	15	45.674027	-0.935123	X	X	X <sup>*</sup>	X	X <sup>*</sup>	X	X	X	X <sup>*</sup>	X <sup>*</sup>	X <sup>*</sup>	X <sup>*</sup>	X <sup>*</sup>	X <sup>*</sup>	X <sup>*</sup>	X	X	X <sup>**</sup>	X <sup>**</sup>	X <sup>**</sup>	X <sup>**</sup>	X <sup>**</sup>	X <sup>**</sup>	X <sup>**</sup>
Perge	01/2008 to 02/2009	monthly	14	44.739868	-1.161181	X	X	X <sup>*</sup>	X	X	X	X	X	X <sup>*</sup>	X <sup>*</sup>	X <sup>*</sup>	X <sup>*</sup>	X <sup>*</sup>	X <sup>*</sup>	X <sup>*</sup>	X	X	X <sup>**</sup>	X <sup>**</sup>	X <sup>**</sup>	X <sup>**</sup>	X <sup>**</sup>	X <sup>**</sup>	X <sup>**</sup>
Renet	02/2008 to 02/2009	bi-monthly	23	44.714466	-1.044013	X	X	X <sup>*</sup>	X	X	X	X	X	X <sup>*</sup>	X <sup>*</sup>	X <sup>*</sup>	X <sup>*</sup>	X <sup>*</sup>	X <sup>*</sup>	X <sup>*</sup>	X	X	X <sup>**</sup>	X <sup>**</sup>	X <sup>**</sup>	X <sup>**</sup>	X <sup>**</sup>	X <sup>**</sup>	X <sup>**</sup>
Milieu	02/2008 to 02/2009	monthly	13	44.697326	-1.022532	X	X	X <sup>*</sup>	X	X	X	X	X	X <sup>*</sup>	X <sup>*</sup>	X <sup>*</sup>	X <sup>*</sup>	X <sup>*</sup>	X <sup>*</sup>	X <sup>*</sup>	X	X	X <sup>**</sup>	X <sup>**</sup>	X <sup>**</sup>	X <sup>**</sup>	X <sup>**</sup>	X <sup>**</sup>	X <sup>**</sup>
Cirés	02/2008 to 02/2009	monthly	13	44.759820	-1.110657	X	X	X <sup>*</sup>	X	X	X	X	X	X <sup>*</sup>	X <sup>*</sup>	X <sup>*</sup>	X <sup>*</sup>	X <sup>*</sup>	X <sup>*</sup>	X <sup>*</sup>	X	X	X <sup>**</sup>	X <sup>**</sup>	X <sup>**</sup>	X <sup>**</sup>	X <sup>**</sup>	X <sup>**</sup>	X <sup>**</sup>
Lanton	02/2008 to 02/2009	monthly	13	44.700283	-1.024385	X	X	X <sup>*</sup>	X	X	X	X	X	X <sup>*</sup>	X <sup>*</sup>	X <sup>*</sup>	X <sup>*</sup>	X <sup>*</sup>	X <sup>*</sup>	X <sup>*</sup>	X	X	X <sup>**</sup>	X <sup>**</sup>	X <sup>**</sup>	X <sup>**</sup>	X <sup>**</sup>	X <sup>**</sup>	X <sup>**</sup>
Targon	02/2008 to 02/2009	bi-monthly	26	44.659049	-0.989050	X	X	X <sup>*</sup>	X	X	X	X	X	X <sup>*</sup>	X <sup>*</sup>	X <sup>*</sup>	X <sup>*</sup>	X <sup>*</sup>	X <sup>*</sup>	X <sup>*</sup>	X	X	X <sup>**</sup>	X <sup>**</sup>	X <sup>**</sup>	X <sup>**</sup>	X <sup>**</sup>	X <sup>**</sup>	X <sup>**</sup>
Landes	02/2008 to 02/2009	monthly	12	44.616912	-1.109066	X	X	X <sup>*</sup>	X	X	X	X	X	X <sup>*</sup>	X <sup>*</sup>	X <sup>*</sup>	X <sup>*</sup>	X <sup>*</sup>	X <sup>*</sup>	X <sup>*</sup>	X	X	X <sup>**</sup>	X <sup>**</sup>	X <sup>**</sup>	X <sup>**</sup>	X <sup>**</sup>	X <sup>**</sup>	X <sup>**</sup>
Layre	02/2008 to 02/2015	bi-monthly or monthly	59	44.626389	-0.996111	X	X	X <sup>*</sup>	X	X <sup>*</sup>	X	X	X	X <sup>*</sup>	X <sup>*</sup>	X <sup>*</sup>	X <sup>*</sup>	X <sup>*</sup>	X <sup>*</sup>	X <sup>*</sup>	X	X	X <sup>**</sup>	X <sup>**</sup>	X <sup>**</sup>	X <sup>**</sup>	X <sup>**</sup>	X <sup>**</sup>	X <sup>**</sup>
Adour	04/2013 to 05/2018	monthly	24	43.498880	-1.294899	X	X	X	X	X	X	X	X	X	X	X	X	X	X	X	X	X	X <sup>**</sup>	X <sup>**</sup>	X <sup>**</sup>	X <sup>**</sup>	X <sup>**</sup>	X <sup>**</sup>	X <sup>**</sup>
Têt	01/2006 to 05/2010	monthly	52	42.713704	2.993488	X	X	X	X	X	X	X	X	X	X	X	X	X	X	X	X	X	X <sup>**</sup>	X <sup>**</sup>	X <sup>**</sup>	X <sup>**</sup>	X <sup>**</sup>	X <sup>**</sup>	X <sup>**</sup>
Aude	01/2006 to 05/2010	monthly	52	43.244281	3.152733	X	X	X	X	X	X	X	X	X	X	X	X	X	X	X	X	X	X <sup>**</sup>	X <sup>**</sup>	X <sup>**</sup>	X <sup>**</sup>	X <sup>**</sup>	X <sup>**</sup>	X <sup>**</sup>
Orb	01/2006 to 05/2010	monthly	52	43.285004	3.281278	X	X	X	X	X	X	X	X	X	X	X	X	X	X	X	X	X	X <sup>**</sup>	X <sup>**</sup>	X <sup>**</sup>	X <sup>**</sup>	X <sup>**</sup>	X <sup>**</sup>	X <sup>**</sup>
Hérault	01/2006 to 05/2010	monthly	52	43.359415	3.435398	X	X	X	X	X	X	X	X	X	X	X	X	X	X	X	X	X	X <sup>**</sup>	X <sup>**</sup>	X <sup>**</sup>	X <sup>**</sup>	X <sup>**</sup>	X <sup>**</sup>	X <sup>**</sup>
Rhône	12/2003 to 01/2011	monthly	105	43.678724	4.621188	X	X	X	X	X	X	X	X	X	X	X	X	X	X	X	X	X	X <sup>**</sup>	X <sup>**</sup>	X <sup>**</sup>	X <sup>**</sup>	X <sup>**</sup>	X <sup>**</sup>	X <sup>**</sup>

698



699  
700  
701  
702  
703  
704  
705  
706  
707  
708  
709  
710  
711  
712  
713  
714  
715

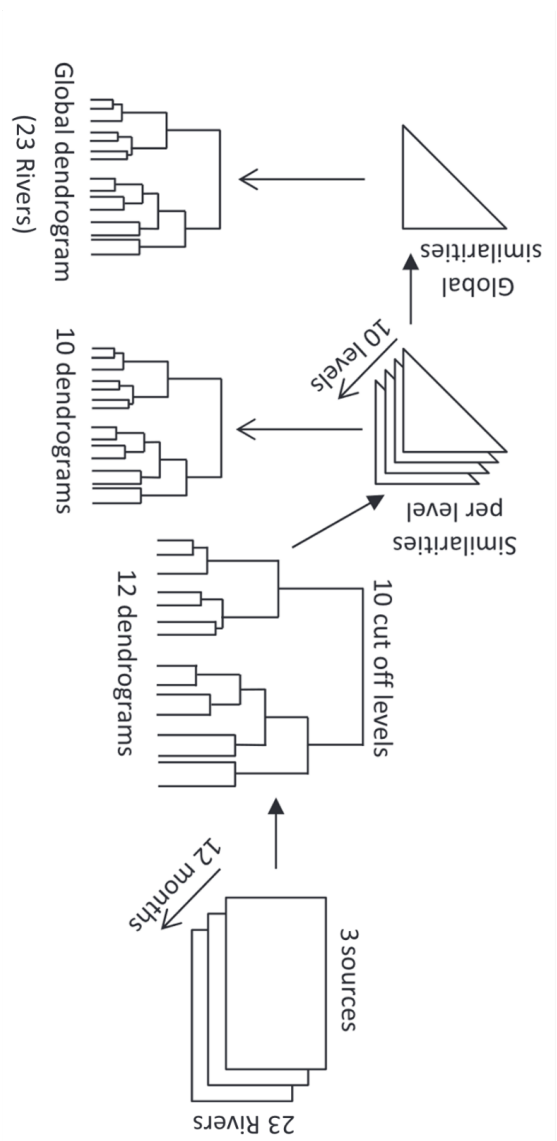
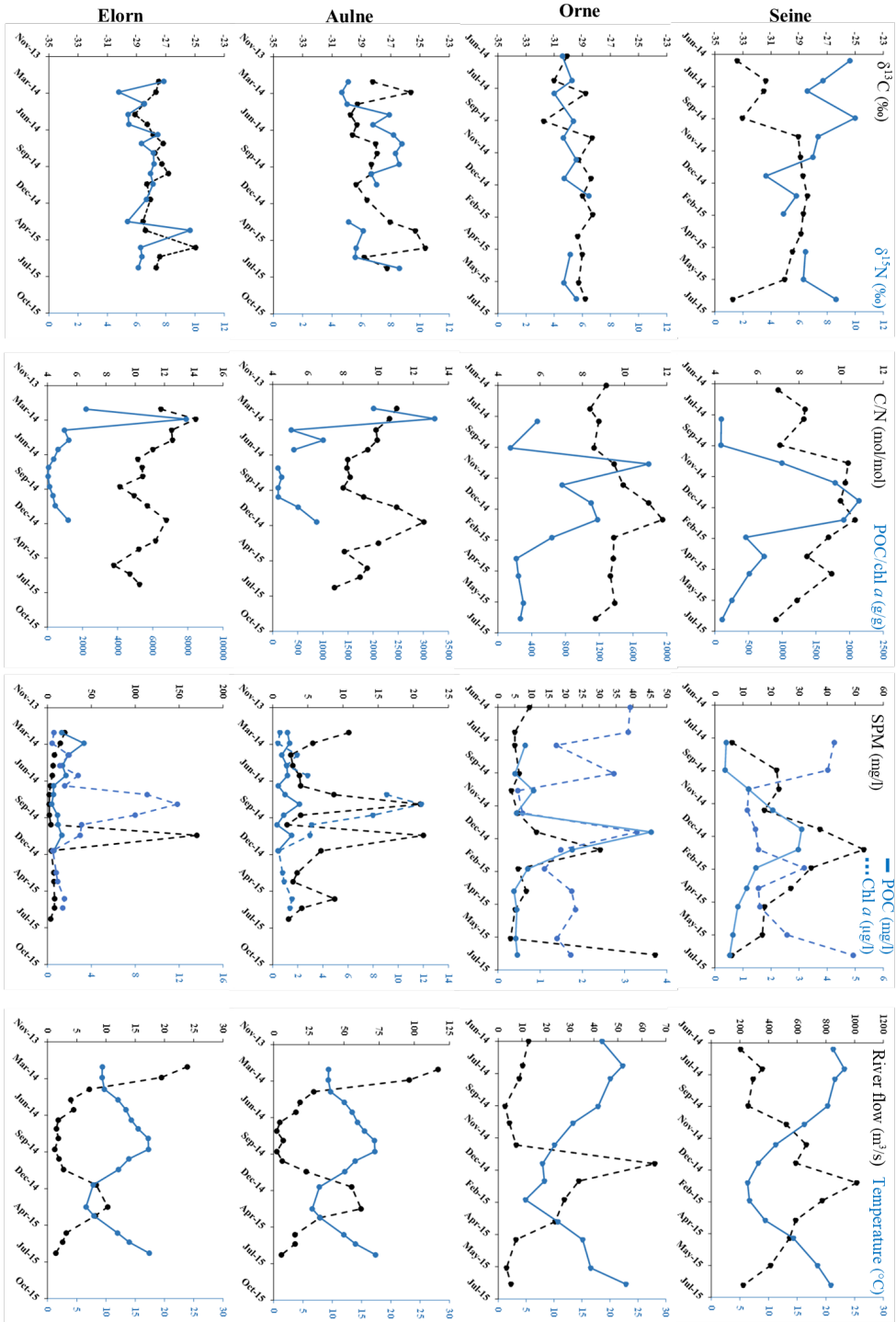


Figure A1 Diagram detailing the regionalization method, adapted from Souissi et al. (2000).





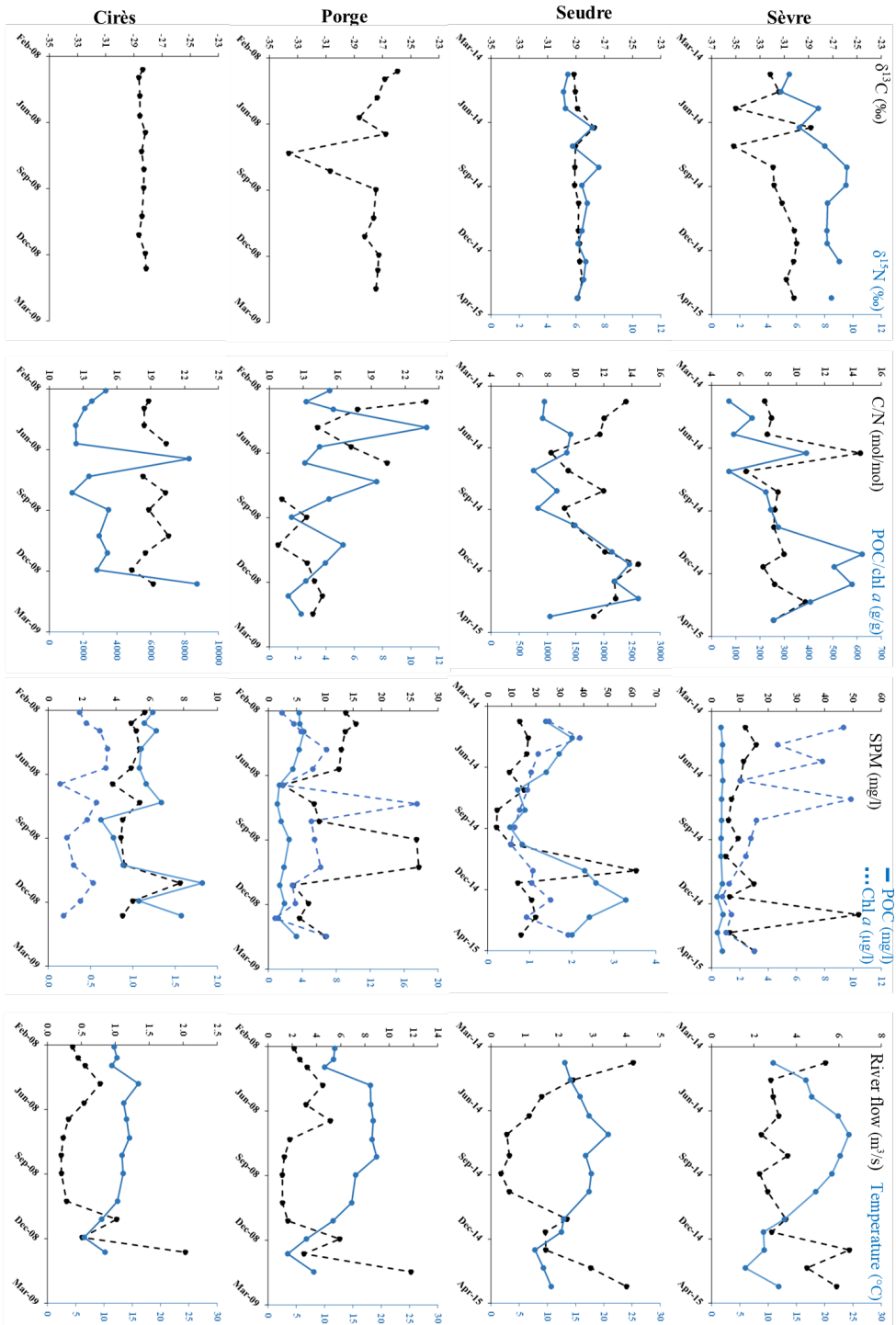
716

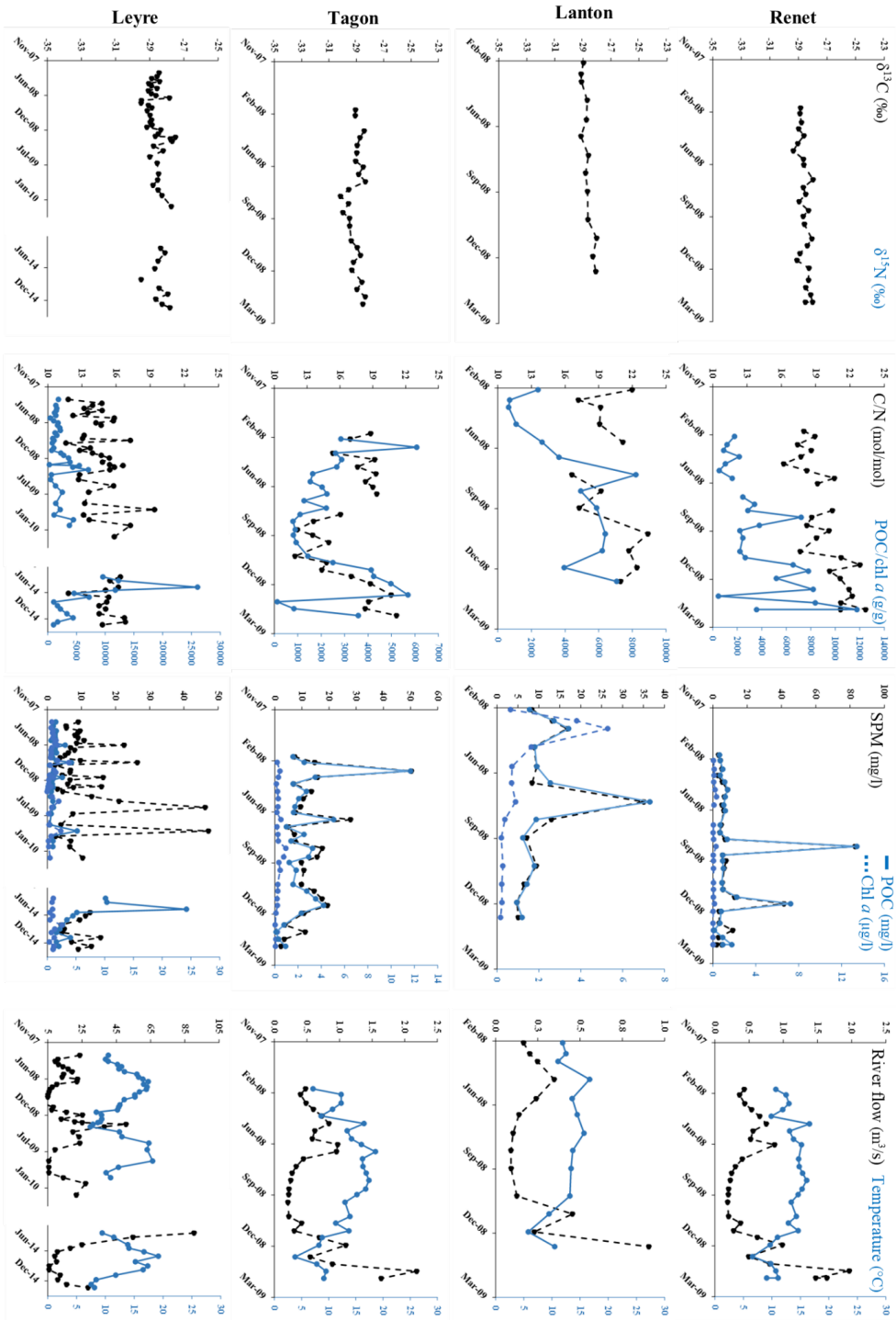


33



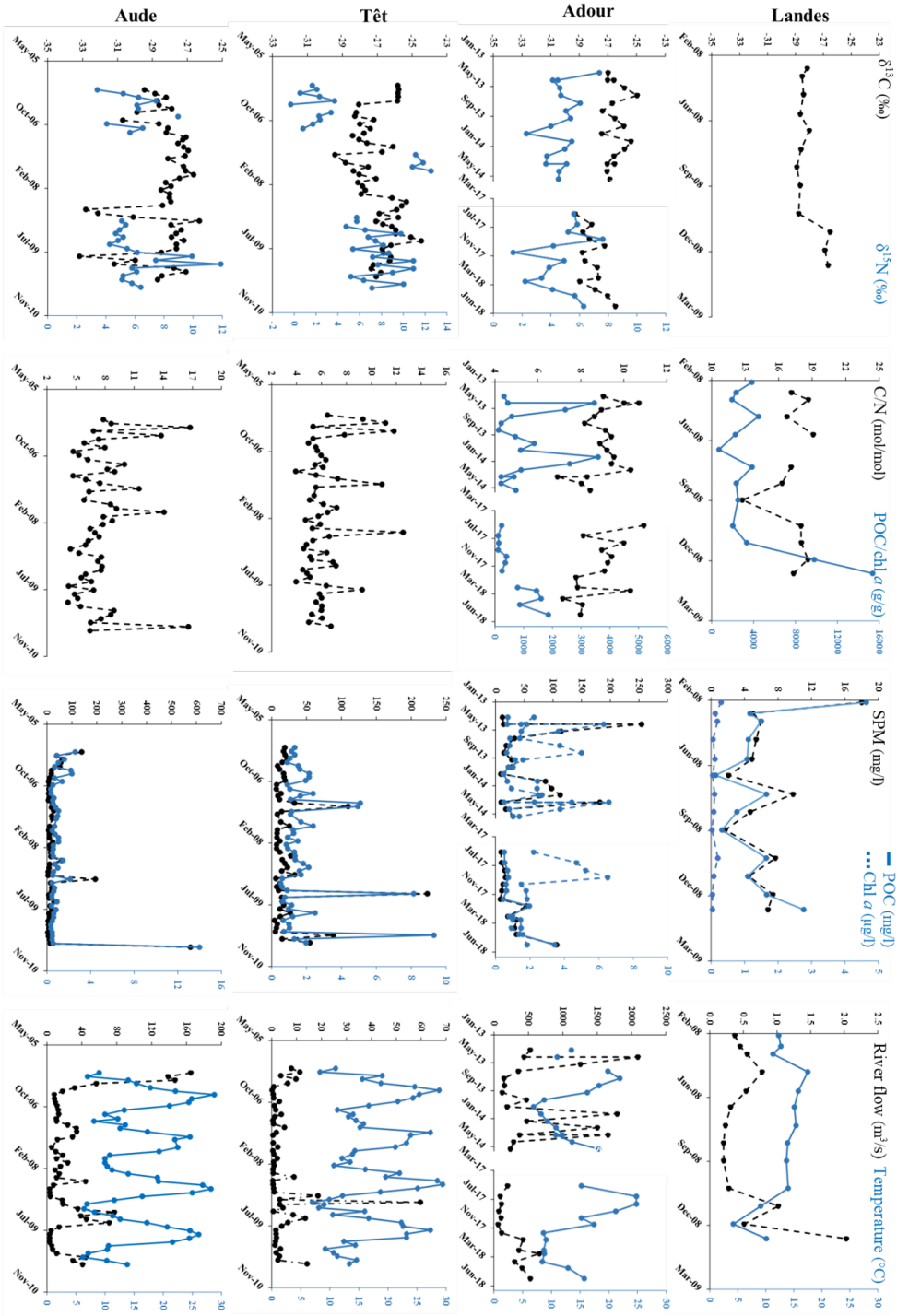
717



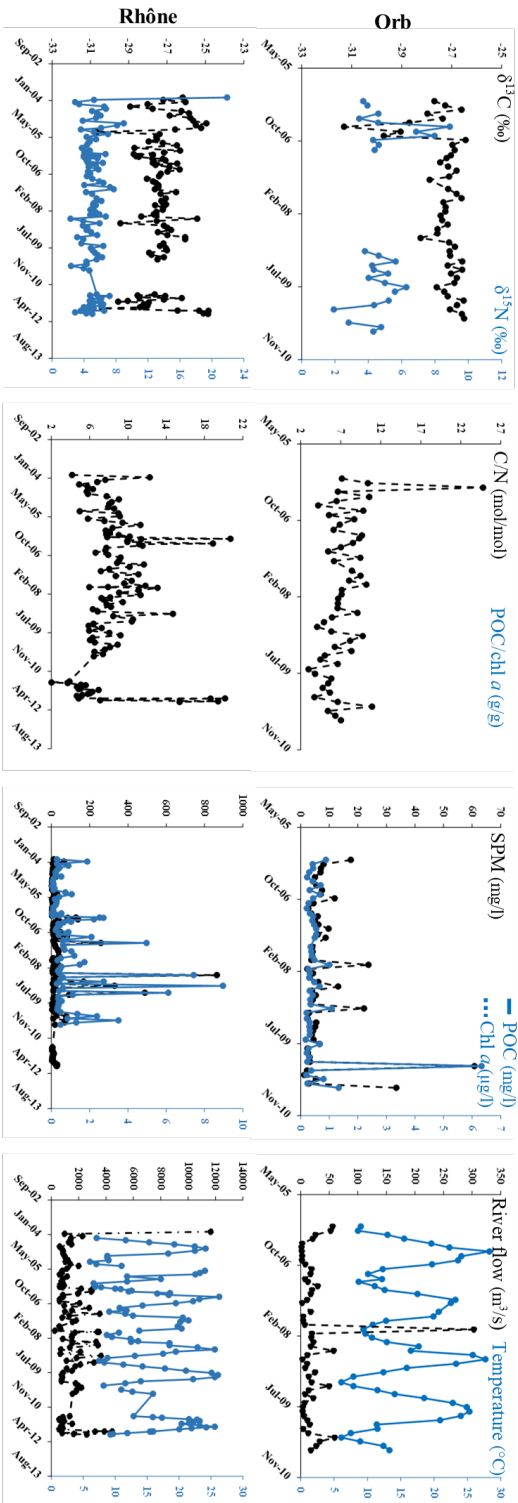




719



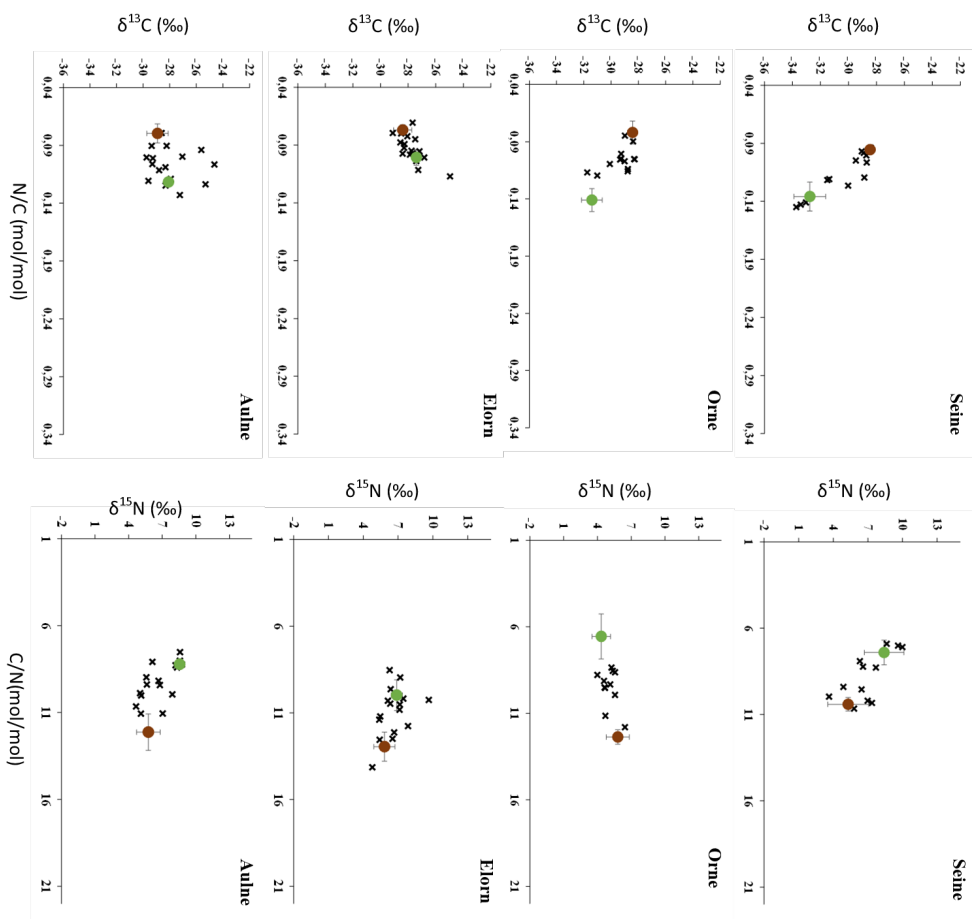
720  
 721  
 722  
 723



724  
 725 **Figure A2** Temporal variations of matter characteristics for representative rivers along the studied periods for  $\delta^{13}\text{C}$  (left axis; black dotted line) and  
 726  $\delta^{15}\text{N}$  (right axis; blue line) (first column); C/N (left axis; black dotted line) and POC/chl a (right axis; blue line) ratios (second column); SPM (left  
 727 axis; black dotted line), POC (right axis; blue line) and chl a (right axis; blue dotted line) concentrations (third column) and river flow (left axis;  
 728 black dotted line) and temperature (right axis; blue line) (fourth column).



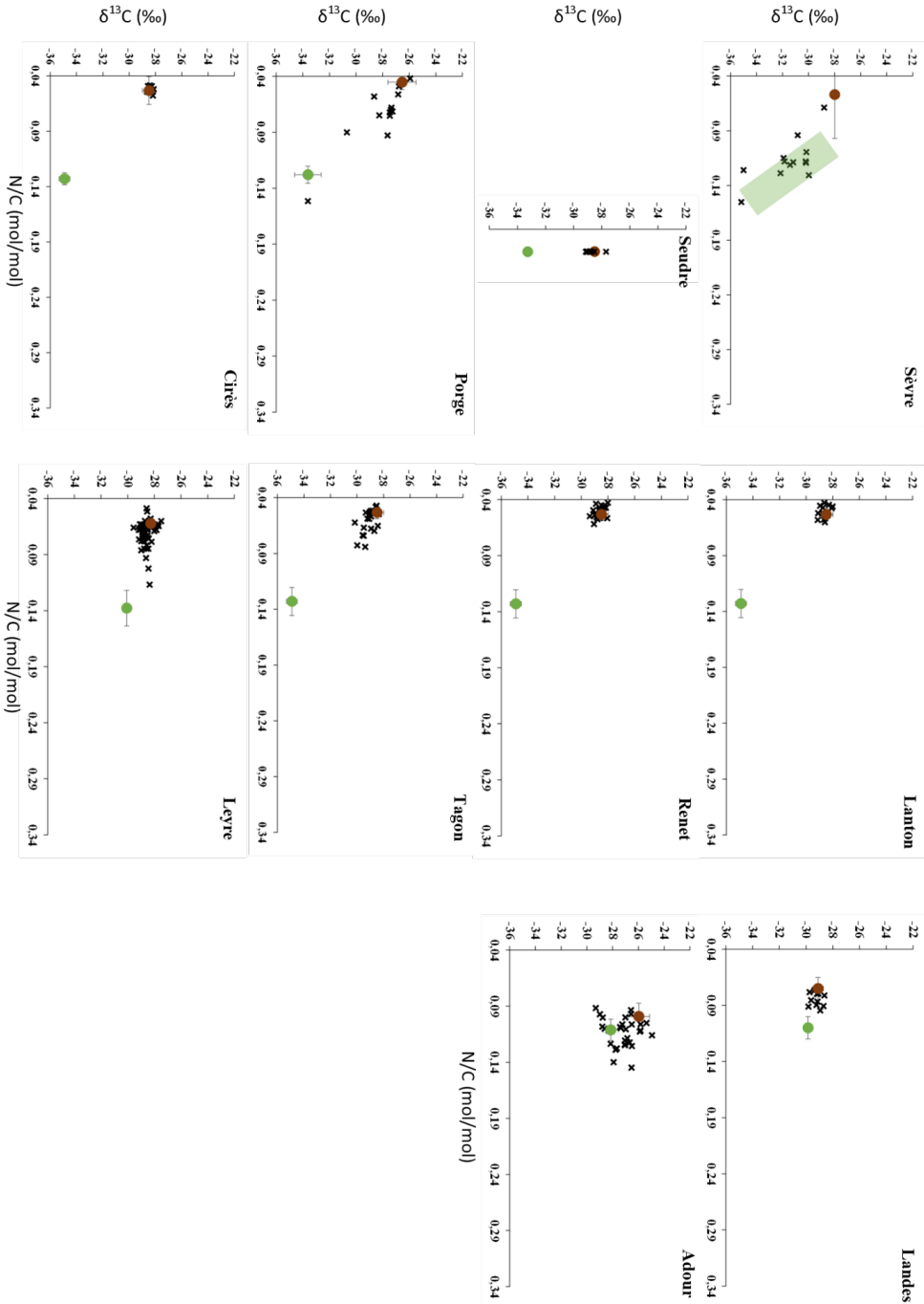
729



38

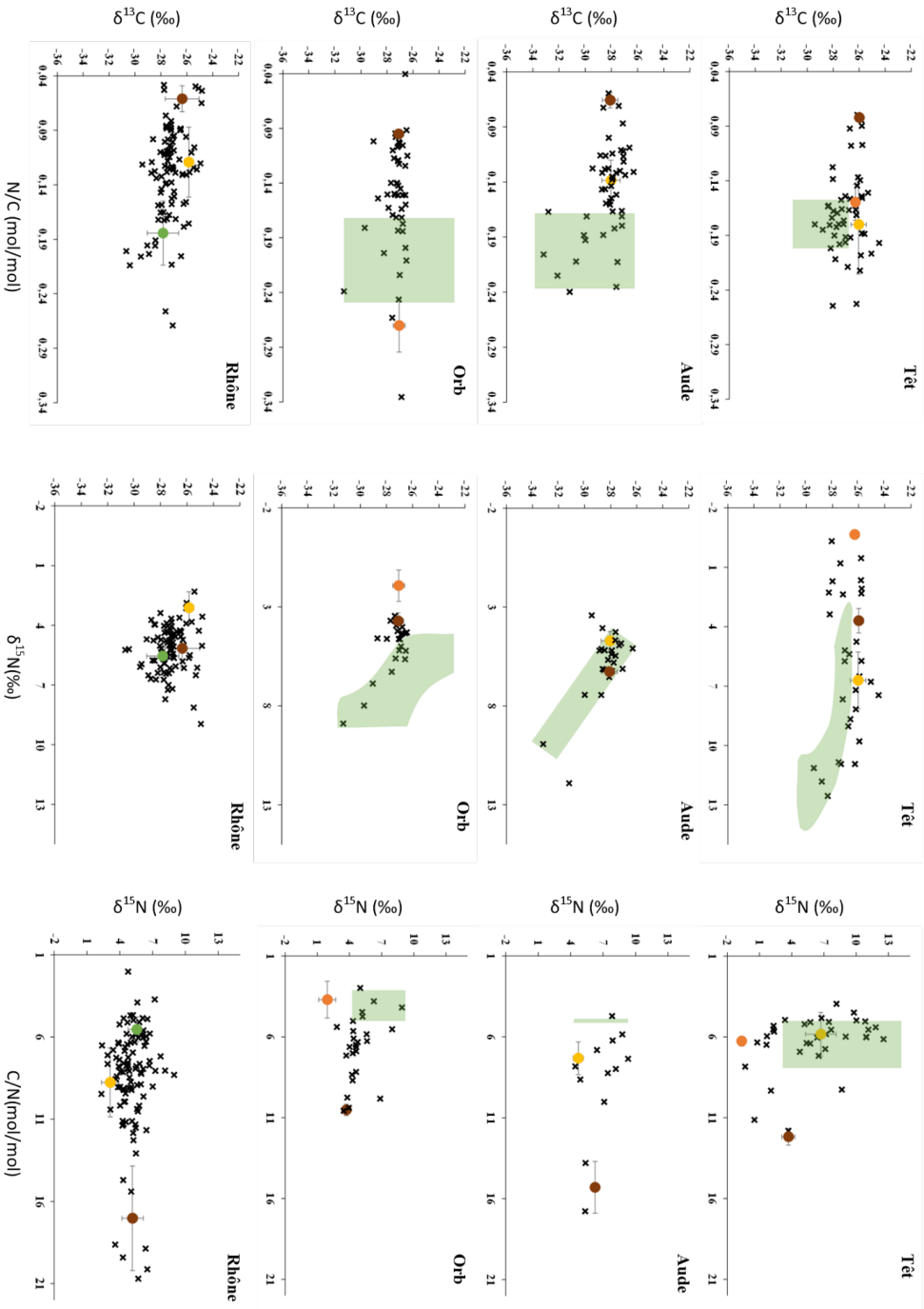


730





731



40



732 Figure A3  $\delta^{13}\text{C}$ ,  $\delta^{15}\text{N}$ , N/C and/or C/N values of bulk POM (black crosses) and sources. The latter are presented as closed circles (average) and  
733 bars (standard deviation) when the signatures were constant over time and by colored area when at least one of the proxies was variable over time  
734 (see Table 2). This colored area corresponds to the dispersion of the values including their uncertainties.





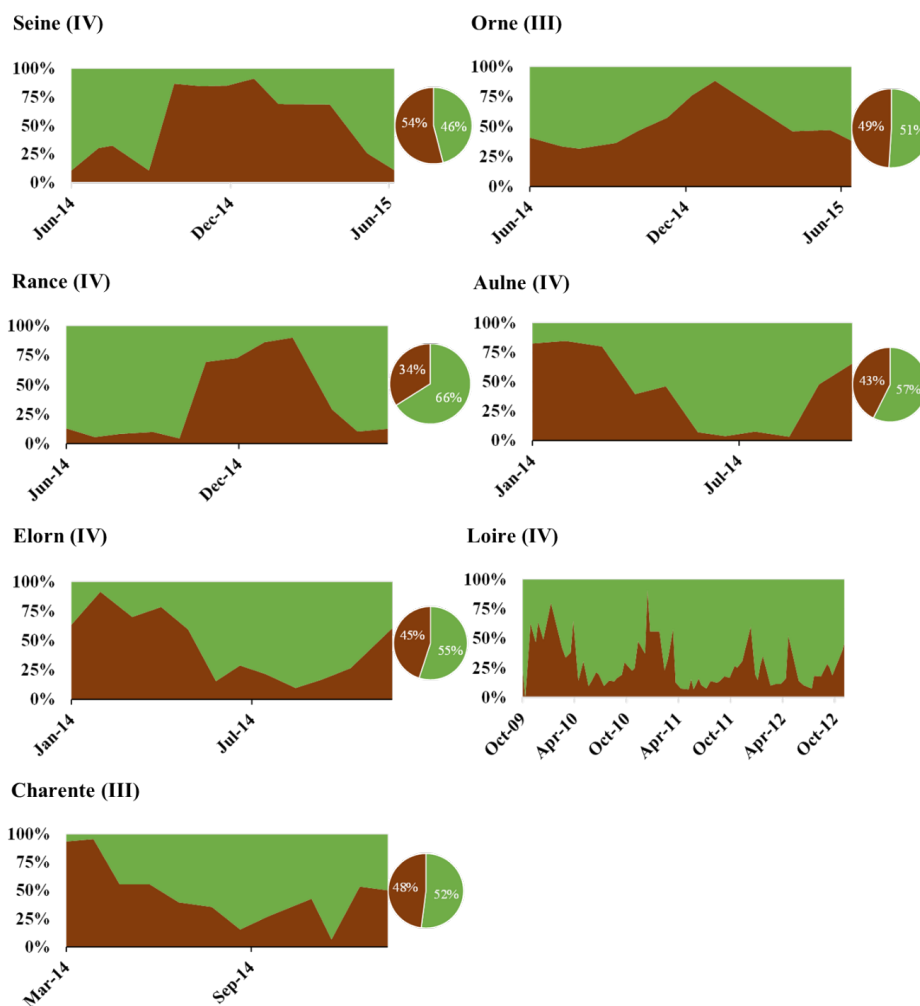
735

736

737

738

739



740 Figure A4 Temporal dynamic (rectangle graphs) and (inter-)annual mean (pie charts) of PN  
741 source proportions. Sources are phytoplankton (green) and labile terrestrial material (brown).

742

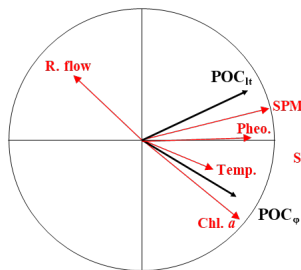
743

744

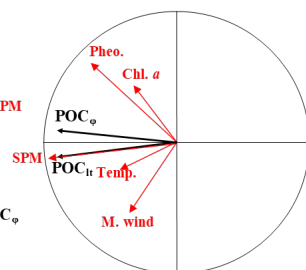


745

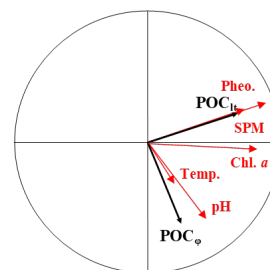
**Tagon (I)**  
*Adj. R<sup>2</sup> 0.70*



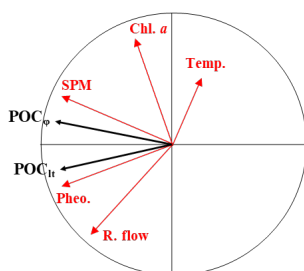
**Lanton (I)**  
*Adj. R<sup>2</sup> 0.93*



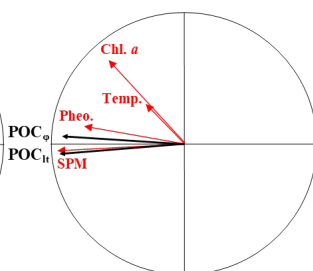
**Leyre (I)**  
*Adj. R<sup>2</sup> 0.41*



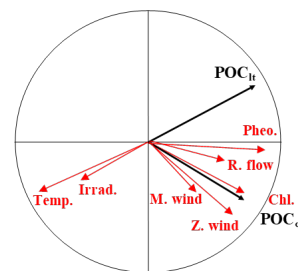
**Cirès (I)**  
*Adj. R<sup>2</sup> 0.74*



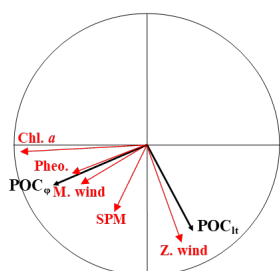
**Renet (I)**  
*Adj. R<sup>2</sup> 0.97*



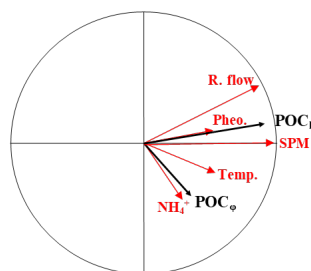
**Seudre (I)**  
*Adj. R<sup>2</sup> 0.72*



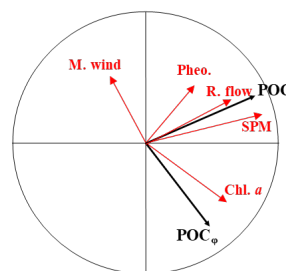
**Porge (II)**  
*Adj. R<sup>2</sup> 0.38*



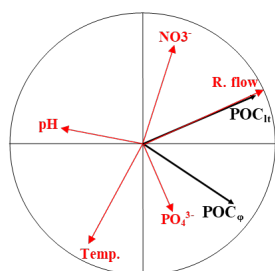
**Adour (II)**  
*Adj. R<sup>2</sup> 0.53*



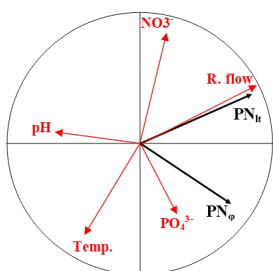
**Landes (II)**  
*Adj. R<sup>2</sup> 0.61*



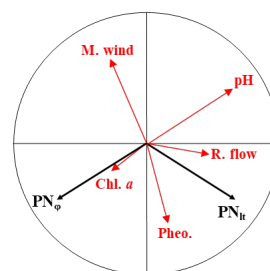
**Orne C (II)**  
*Adj. R<sup>2</sup> 0.72*



**Orne N (II)**  
*Adj. R<sup>2</sup> 0.74*



**Charente N (II)**  
*Adj. R<sup>2</sup> 0.43*



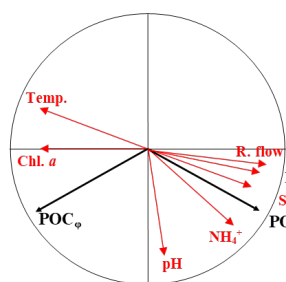
746

747

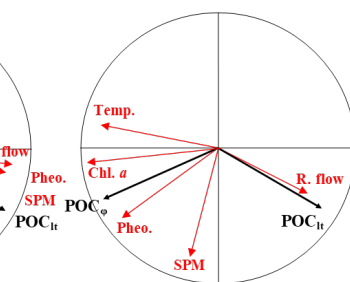


748  
749  
750  
751

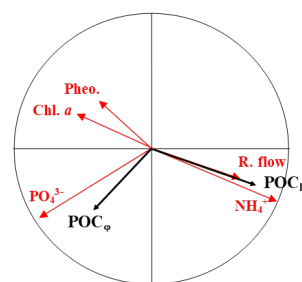
**Seine C (IV)**  
*Adj. R<sup>2</sup> 0.95*



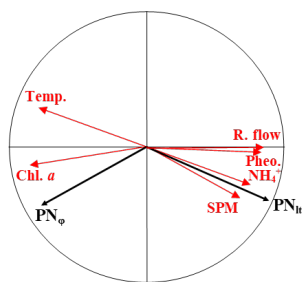
**Aulne C (IV)**  
*Adj. R<sup>2</sup> 0.82*



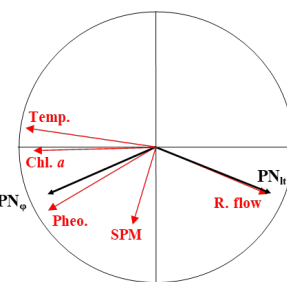
**Elorn C (IV)**  
*Adj. R<sup>2</sup> 0.23*



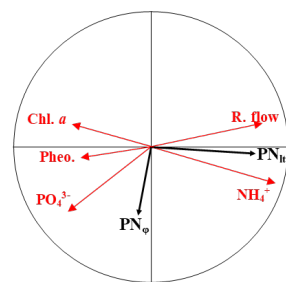
**Seine N (IV)**  
*Adj. R<sup>2</sup> 0.80*



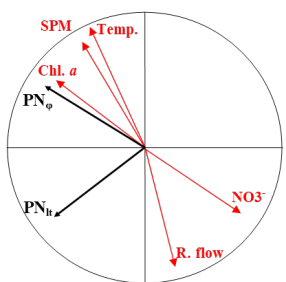
**Aulne N (IV)**  
*Adj. R<sup>2</sup> 0.74*



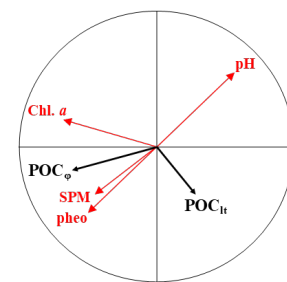
**Elorn N (IV)**  
*Adj. R<sup>2</sup> 0.04*



**Rance N (IV)**  
*Adj. R<sup>2</sup> 0.56*



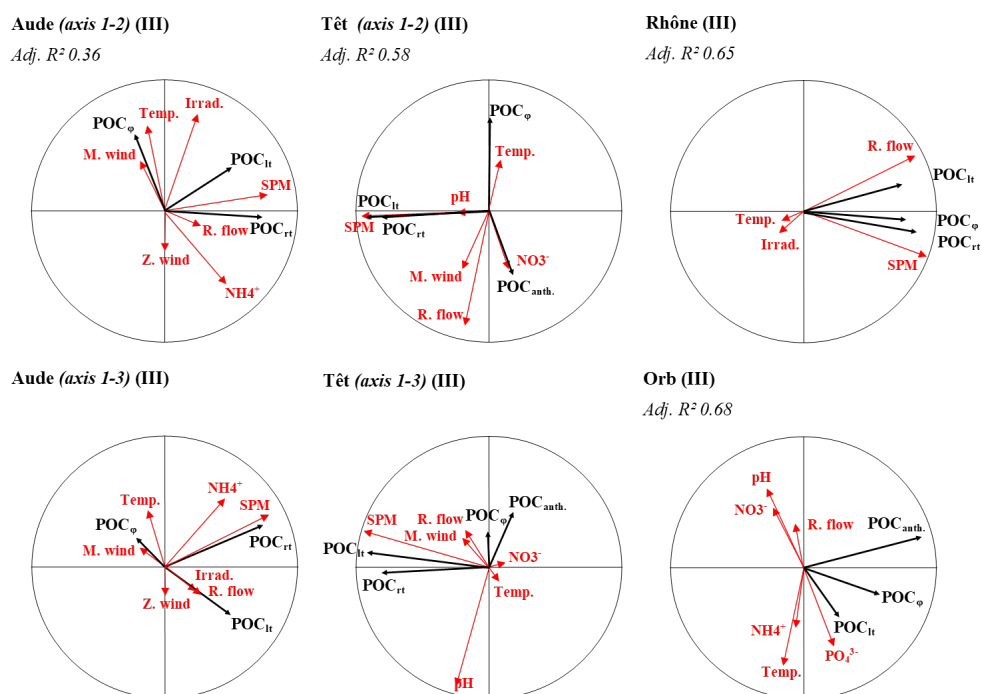
**Sèvre (IV)**  
*Adj. R<sup>2</sup> 0.01*



752  
753  
754  
755



756  
 757  
 758  
 759  
 760  
 761  
 762  
 763



764

765 **Figure A5** Redundancy analyses (correlation circles) of rivers standing for each type of river.  
 766 Black arrows represent explained variables (concentration of POC or PN sources) and red  
 767 arrows represent explaining variables (environmental variables). River types are recalled  
 768 (Roman numerals). POC or PN<sub>lt</sub> = Labile terrestrial POC or PN; POC<sub>rt</sub> = Refractory terrestrial  
 769 POC; POC or PN<sub>φ</sub> = Phytoplankton POC or PN; POC<sub>anth.</sub> = Anthropic POC; SPM =  
 770 Suspended Particulate Matter; POC or PN = Particulate Organic Carbon or nitrogen; Chl. a =  
 771 Chlorophyll a; Pheo. = Phaeopigments; R. flow = River flow; Temp. = Temperature; M. wind  
 772 = Meridional wind; Z. wind = Zonal wind; Irrad. = Irradiance; NH<sub>4</sub><sup>+</sup> = Ammonium; NO<sub>3</sub><sup>-</sup> =  
 773 Nitrate; PO<sub>4</sub><sup>3-</sup> = Phosphate; *Adj. R<sup>2</sup>* = adjusted R<sup>2</sup>.



774

### 775 **Author contributions**

776 FF: Formal analysis, Investigation, Visualization, Writing – original draft. CL: Formal analysis,  
777 Conceptualization, Supervision, Writing – original draft, Writing – review & editing. KC:  
778 Investigation. JD: Investigation, Visualization, Writing – review & editing. MG: Investigation.  
779 PK: Investigation. PP: Investigation, Visualization, Writing – review & editing.

780 NS: Conceptualization, Formal analysis, Investigation, Methodology, Supervision, Writing –  
781 original draft, Writing – review & editing.

782

### 783 **Competing interest**

784 The authors declare that they have no known competing financial interests or personal  
785 relationships that could have appeared to influence the work reported in this paper.

786

### 787 **Data availability**

788 All POM and environmental data used in this article are stored in Figshare, accessible for the  
789 review process through this private link : <https://figshare.com/s/a7101028e6ab5452c4db>.

790

### 791 **References**

792 Arellano, A. R., Bianchi, T. S., Osburn, C. L., D'Sa, E. J., Ward, N. D., Oviedo-Vargas, D.,  
793 Joshi, I. D., Ko, D. S., Shields, M. R., Kurian, G., and Green, J.: Mechanisms of Organic  
794 Matter Export in Estuaries with Contrasting Carbon Sources, *Journal of Geophysical*  
795 *Research: Biogeosciences*, 124, 3168–3188, <https://doi.org/10.1029/2018JG004868>, 2019.

796 Barros, G. V., Martinelli, L. A., Oliveira Novais, T. M., Ometto, J. P. H. B., and Zuppi, G.  
797 M.: Stable isotopes of bulk organic matter to trace carbon and nitrogen dynamics in an  
798 estuarine ecosystem in Babitonga Bay (Santa Catarina, Brazil), *Science of The Total*  
799 *Environment*, 408, 2226–2232, <https://doi.org/10.1016/j.scitotenv.2010.01.060>, 2010.

800 Bate, G. C., Whitfield, A. K., Adams, J. B., Huizinga, P., and Wooldridge, T. H.: The  
801 importance of the river-estuary interface (REI) zone in estuaries, *Water SA*, 28, 271–280,  
802 <https://doi.org/10.4314/wsa.v28i3.4894>, 2002.

803 Bonin, P., Prime, A.-H., Galeron, M.-A., Guasco, S., and Rontani, J.-F.: Enhanced biotic  
804 degradation of terrestrial POM in an estuarine salinity gradient: interactive effects of organic  
805 matter pools and changes of bacterial communities, *Aquatic Microbial Ecology*, 83, 147–159,  
806 <https://doi.org/10.3354/ame01908>, 2019.

807 Borcard, D., Legendre, P., and Gillet, F.: *Numerical Ecology with R*, Springer, 315 pp., 2011.



- 808 Bouwman, L., Beusen, A., Glibert, P. M., Overbeek, C., Pawlowski, M., Herrera, J., Mulsow,  
809 S., Yu, R., and Zhou, M.: Mariculture: significant and expanding cause of coastal nutrient  
810 enrichment, *Environ. Res. Lett.*, 8, 044026, <https://doi.org/10.1088/1748-9326/8/4/044026>,  
811 2013.
- 812 Brett, M. T., Bunn, S. E., Chandra, S., Galloway, A. W. E., Guo, F., Kainz, M. J., Kankaala,  
813 P., Lau, D. C. P., Moulton, T. P., Power, M. E., Rasmussen, J. B., Taipale, S. J., Thorp, J. H.,  
814 and Wehr, J. D.: How important are terrestrial organic carbon inputs for secondary production  
815 in freshwater ecosystems?, *Freshwater Biology*, 62, 833–853,  
816 <https://doi.org/10.1111/fwb.12909>, 2017.
- 817 Canton, M., Anschutz, P., Coynel, A., Polsenaere, P., Auby, I., and Poirier, D.: Nutrient  
818 export to an Eastern Atlantic coastal zone: first modeling and nitrogen mass balance,  
819 *Biogeochemistry*, 107, 361–377, <https://doi.org/10.1007/s10533-010-9558-7>, 2012.
- 820 Canuel, E. A. and Hardison, A. K.: Sources, Ages, and Alteration of Organic Matter in  
821 Estuaries, *Annual Review of Marine Science*, 8, 409–434, <https://doi.org/10.1146/annurev-marine-122414-034058>, 2016.
- 823 Cathalot, C., Rabouille, C., Tisnérat-Laborde, N., Toussaint, F., Kerhervé, P., Buscail, R.,  
824 Loftis, K., Sun, M.-Y., Tronczynski, J., Azoury, S., Lansard, B., Treignier, C., Pastor, L., and  
825 Tesi, T.: The fate of river organic carbon in coastal areas: A study in the Rhône River delta  
826 using multiple isotopic ( $\delta^{13}\text{C}$ ,  $\Delta^{14}\text{C}$ ) and organic tracers, *Geochimica et Cosmochimica*  
827 *Acta*, 118, 33–55, <https://doi.org/10.1016/j.gca.2013.05.001>, 2013.
- 828 Chevalier, N., Savoye, N., Dubois, S., Lama, M. L., David, V., Lecroart, P., le Ménach, K.,  
829 and Budzinski, H.: Precise indices based on *n*-alkane distribution for quantifying sources of  
830 sedimentary organic matter in coastal systems, *Organic Geochemistry*, 88, 69–77,  
831 <https://doi.org/10.1016/j.orggeochem.2015.07.006>, 2015.
- 832 Codiga, D. L., Stoffel, H. E., Oviatt, C. A., and Schmidt, C. E.: Managed Nitrogen Load  
833 Decrease Reduces Chlorophyll and Hypoxia in Warming Temperate Urban Estuary, *Frontiers*  
834 *in Marine Science*, 9, 2022.
- 835 Copard, Y., Eyrolle, F., Grosbois, C., Lepage, H., Ducros, L., Morereau, A., Bodereau, N.,  
836 Cossonnet, C., and Desmet, M.: The unravelling of radiocarbon composition of organic  
837 carbon in river sediments to document past anthropogenic impacts on river systems, *Science*  
838 *of The Total Environment*, 806, 150890, <https://doi.org/10.1016/j.scitotenv.2021.150890>,  
839 2022.
- 840 Dagg, M., Benner, R., Lohrenz, S., and Lawrence, D.: Transformation of dissolved and  
841 particulate materials on continental shelves influenced by large rivers: plume processes,  
842 *Continental Shelf Research*, 24, 833–858, <https://doi.org/10.1016/j.csr.2004.02.003>, 2004.
- 843 Dalzell, B. J., Filley, T. R., and Harbor, J. M.: The role of hydrology in annual organic carbon  
844 loads and terrestrial organic matter export from a midwestern agricultural watershed,  
845 *Geochimica et Cosmochimica Acta*, 71, 1448–1462,  
846 <https://doi.org/10.1016/j.gca.2006.12.009>, 2007.
- 847 David, V., Sautour, B., Chardy, P., and Leconte, M.: Long-term changes of the zooplankton  
848 variability in a turbid environment: The Gironde estuary (France), *Estuarine, Coastal and*  
849 *Shelf Science*, 64, 171–184, <https://doi.org/10.1016/j.ecss.2005.01.014>, 2005.



- 850 Deborde, J.: Dynamique des sels nutritifs et de la matière organique dans le système  
851 fluvioestuarien de l'Adour/Golfe de Gascogne, Université de Pau et des Pays de l'adour,  
852 2019.
- 853 Descy, J.-P., Leitaó, M., Everbecq, E., Smitz, J. S., and Deliège, J.-F.: Phytoplankton of the  
854 River Loire, France: a biodiversity and modelling study, *Journal of Plankton Research*, 34,  
855 120–135, <https://doi.org/10.1093/plankt/fbr085>, 2012.
- 856 Dodds, W. K. and Smith, V. H.: Nitrogen, phosphorus, and eutrophication in streams, *Inland  
857 Waters*, 6, 155–164, <https://doi.org/10.5268/IW-6.2.909>, 2016.
- 858 Dubois, S., Savoye, N., Grémare, A., Plus, M., Charlier, K., Beltoise, A., and Blanchet, H.:  
859 Origin and composition of sediment organic matter in a coastal semi-enclosed ecosystem: An  
860 elemental and isotopic study at the ecosystem space scale, *Journal of Marine Systems*, 94, 64–  
861 73, <https://doi.org/10.1016/j.jmarsys.2011.10.009>, 2012.
- 862 Dunn†, J. C.: Well-Separated Clusters and Optimal Fuzzy Partitions, *Journal of Cybernetics*,  
863 4, 95–104, <https://doi.org/10.1080/01969727408546059>, 1974.
- 864 Dürr, H. H., Laruelle, G. G., van Kempen, C. M., Slomp, C. P., Meybeck, M., and  
865 Middelkoop, H.: Worldwide Typology of Nearshore Coastal Systems: Defining the Estuarine  
866 Filter of River Inputs to the Oceans, *Estuaries and Coasts*, 34, 441–458,  
867 <https://doi.org/10.1007/s12237-011-9381-y>, 2011.
- 868 Etcheber, H., Taillez, A., Abril, G., Garnier, J., Servais, P., Moatar, F., and Commarieu, M.-  
869 V.: Particulate organic carbon in the estuarine turbidity maxima of the Gironde, Loire and  
870 Seine estuaries: origin and lability, *Hydrobiologia*, 588, 245–259,  
871 <https://doi.org/10.1007/s10750-007-0667-9>, 2007.
- 872 Falkowski, P. G., Barber, R. T., and Smetacek, V.: Biogeochemical Controls and Feedbacks  
873 on Ocean Primary Production, *Science*, 281, 200–206,  
874 <https://doi.org/10.1126/science.281.5374.200>, 1998.
- 875 Ferchiche, F., Liénart, C., Charlier, K., Coynel, A., Gorse-Labadie, L., and Savoye, N.:  
876 Quantifying particulate organic matter: source composition and fluxes at the river-estuary  
877 interface, *Front. Freshw. Sci.*, 2, <https://doi.org/10.3389/ffwsc.2024.1437431>, 2024.
- 878 Ferchiche, F., Liénart, C., Savoye, N., and Wassenaar, L. I.: Unlocking the potential of  
879 hydrogen isotopes ( $\delta^2\text{H}$ ) in tracing riverine particulate organic matter sources and dynamics,  
880 *Aquat Sci*, 87, 5, <https://doi.org/10.1007/s00027-024-01127-1>, 2025.
- 881 Fernandez, I., Mahieu, N., and Cadisch, G.: Carbon isotopic fractionation during  
882 decomposition of plant materials of different quality, *Global Biogeochemical Cycles*, 17,  
883 <https://doi.org/10.1029/2001GB001834>, 2003.
- 884 Field, C. B., Behrenfeld, M. J., Randerson, J. T., and Falkowski, P.: Primary Production of the  
885 Biosphere: Integrating Terrestrial and Oceanic Components, *Science*, 281, 237–240,  
886 <https://doi.org/10.1126/science.281.5374.237>, 1998.
- 887 Finlay, J. C., Doucett, R. R., and McNEELY, C.: Tracing energy flow in stream food webs  
888 using stable isotopes of hydrogen, *Freshwater Biology*, 55, 941–951,  
889 <https://doi.org/10.1111/j.1365-2427.2009.02327.x>, 2010.





- 890 Fry, B.:  $^{13}\text{C}/^{12}\text{C}$  fractionation by marine diatoms, *Marine Ecology Progress Series*, 134,  
891 283–294, <https://doi.org/10.3354/meps134283>, 1996.
- 892 Galeron, M.-A., Radakovitch, O., Charrière, B., Vaultier, F., and Rontani, J.-F.: Autoxidation  
893 as a major player in the fate of terrestrial particulate organic matter in seawater, *Journal of*  
894 *Geophysical Research: Biogeosciences*, 122, 1203–1215,  
895 <https://doi.org/10.1002/2016JG003708>, 2017.
- 896 Gawade, L., Krishna, M. S., Sarma, V. V. S. S., Hemalatha, K. P. J., and Venkateshwara Rao,  
897 Y.: Spatio-temporal variability in the sources of particulate organic carbon and nitrogen in a  
898 tropical Godavari estuary, *Estuarine, Coastal and Shelf Science*, 215, 20–29,  
899 <https://doi.org/10.1016/j.ecss.2018.10.004>, 2018.
- 900 Golubkov, M. S., Nikulina, V. N., Tiunov, A. V., and Golubkov, S. M.: Stable C and N  
901 Isotope Composition of Suspended Particulate Organic Matter in the Neva Estuary: The Role  
902 of Abiotic Factors, Productivity, and Phytoplankton Taxonomic Composition, *Journal of*  
903 *Marine Science and Engineering*, 8, 959, <https://doi.org/10.3390/jmse8120959>, 2020.
- 904 Goñi, M. A., Voulgaris, G., and Kim, Y. H.: Composition and fluxes of particulate organic  
905 matter in a temperate estuary (Winyah Bay, South Carolina, USA) under contrasting physical  
906 forcings, *Estuarine, Coastal and Shelf Science*, 85, 273–291,  
907 <https://doi.org/10.1016/j.ecss.2009.08.013>, 2009.
- 908 Govan, E. and Parnell, A.: *simmr: A Stable Isotope Mixing Model*, 2023.
- 909 Grunicke, F., Wagner, A., von Elert, E., Weitere, M., and Berendonk, T.: Riparian detritus vs.  
910 stream detritus: food quality determines fitness of juveniles of the highly endangered  
911 freshwater pearl mussels (*Margaritifera margaritifera*), *Hydrobiologia*, 850, 729–746,  
912 <https://doi.org/10.1007/s10750-022-05120-3>, 2023.
- 913 Harmelin-Vivien, M., Dierking, J., Bănar, D., Fontaine, M. F., and Arlhac, D.: Seasonal  
914 variation in stable C and N isotope ratios of the Rhone River inputs to the Mediterranean Sea  
915 (2004–2005), *Biogeochemistry*, 100, 139–150, <https://doi.org/10.1007/s10533-010-9411-z>,  
916 2010.
- 917 Hellings, L., Dehairs, F., Tackx, M., Keppens, E., and Baeyens, W.: Origin and fate of  
918 organic carbon in the freshwater part of the Scheldt Estuary as traced by stable carbon isotope  
919 composition, *Biogeochemistry*, 47, 167–186, <https://doi.org/10.1023/A:1006143827118>,  
920 1999.
- 921 Higuera, M., Kerhervé, P., Sanchez-Vidal, A., Calafat, A., Ludwig, W., Verdoit-Jarraya, M.,  
922 Heussner, S., and Canals, M.: Biogeochemical characterization of the riverine particulate  
923 organic matter transferred to the NW Mediterranean Sea, *Biogeosciences*, 11, 157–172,  
924 <https://doi.org/10.5194/bg-11-157-2014>, 2014.
- 925 Hilton, R. G., Galy, A., Hovius, N., Horng, M.-J., and Chen, H.: The isotopic composition of  
926 particulate organic carbon in mountain rivers of Taiwan, *Geochimica et Cosmochimica Acta*,  
927 74, 3164–3181, <https://doi.org/10.1016/j.gca.2010.03.004>, 2010.
- 928 Hou, P., Eglinton, T. I., Yu, M., Montluçon, D. B., Haghypour, N., Zhang, H., Jin, G., and  
929 Zhao, M.: Degradation and Aging of Terrestrial Organic Carbon within Estuaries:



- 930 Biogeochemical and Environmental Implications, *Environmental Science and Technology*,  
931 55, 10852–10861, <https://doi.org/10.1021/acs.est.1c02742>, 2021.
- 932 Hounshell, A. G., Fegley, S. R., Hall, N. S., Osburn, C. L., and Paerl, H. W.: Riverine  
933 Discharge and Phytoplankton Biomass Control Dissolved and Particulate Organic Matter  
934 Dynamics over Spatial and Temporal Scales in the Neuse River Estuary, North Carolina,  
935 *Estuaries and Coasts*, 45, 96–113, <https://doi.org/10/gj64px>, 2022.
- 936 Kang, S., Kim, J.-H., Joe, Y. J., Jang, K., Nam, S.-I., and Shin, K.-H.: Long-term  
937 environmental changes in the Geum Estuary (South Korea): Implications of river  
938 impoundments, *Marine Pollution Bulletin*, 168, 112383, <https://doi.org/10/gnpb2t>, 2021.
- 939 Ke, Z., Tan, Y., Huang, L., Liu, J., Xiang, C., Zhao, C., and Zhang, J.: Significantly depleted  
940 <sup>15</sup>N in suspended particulate organic matter indicating a strong influence of sewage loading  
941 in Daya Bay, China, *Science of The Total Environment*, 650, 759–768,  
942 <https://doi.org/10.1016/j.scitotenv.2018.09.076>, 2019.
- 943 Kelso, J. E. and Baker, M. A.: Organic Matter Is a Mixture of Terrestrial, Autochthonous, and  
944 Wastewater Effluent in an Urban River, *Frontiers in Environmental Science*, 7,  
945 <https://doi.org/10.3389/fenvs.2019.00202>, 2020.
- 946 Kelso, J. E. and Baker, M. A.: Organic matter sources and composition in four watersheds  
947 with mixed land cover, *Hydrobiologia*, 849, 2663–2682, <https://doi.org/10.1007/s10750-022-04884-y>, 2022.
- 949 Kendall, C., Silva, S. R., and Kelly, V. J.: Carbon and nitrogen isotopic compositions of  
950 particulate organic matter in four large river systems across the United States, *Hydrological  
951 Processes*, 15, 1301–1346, <https://doi.org/10.1002/hyp.216>, 2001.
- 952 Khan, M. N. and Mohammad, F.: Eutrophication: Challenges and Solutions, in:  
953 Eutrophication: Causes, Consequences and Control: Volume 2, edited by: Ansari, A. A. and  
954 Gill, S. S., Springer Netherlands, Dordrecht, 1–15, [https://doi.org/10.1007/978-94-007-7814-6\\_1](https://doi.org/10.1007/978-94-007-7814-6_1), 2014.
- 956 Lambert, T., Bouillon, S., Darchambeau, F., Morana, C., Roland, F. A. E., Descy, J.-P., and  
957 Borges, A. V.: Effects of human land use on the terrestrial and aquatic sources of fluvial  
958 organic matter in a temperate river basin (The Meuse River, Belgium), *Biogeochemistry*, 136,  
959 191–211, <https://doi.org/10.1007/s10533-017-0387-9>, 2017.
- 960 Lebreton, B., Beseres Pollack, J., Blomberg, B., Palmer, T. A., Adams, L., Guillou, G., and  
961 Montagna, P. A.: Origin, composition and quality of suspended particulate organic matter in  
962 relation to freshwater inflow in a South Texas estuary, *Estuarine, Coastal and Shelf Science*,  
963 170, 70–82, <https://doi.org/10.1016/j.ecss.2015.12.024>, 2016.
- 964 Legendre, P., Oksanen, J., and ter Braak, C. J. F.: Testing the significance of canonical axes in  
965 redundancy analysis, *Methods in Ecology and Evolution*, 2, 269–277,  
966 <https://doi.org/10.1111/j.2041-210X.2010.00078.x>, 2011.
- 967 Lheureux, A., David, V., Del Amo, Y., Soudant, D., Auby, I., Ganthy, F., Blanchet, H.,  
968 Cordier, M.-A., Costes, L., Ferreira, S., Mornet, L., Nowaczyk, A., Parra, M., D'Amico, F.,  
969 Gouriou, L., Meteigner, C., Oger-Jeanneret, H., Rigouin, L., Rumebe, M., Tournaire, M.-P.,  
970 Trut, F., Trut, G., and Savoye, N.: Bi-decadal changes in nutrient concentrations and ratios in



- 971 marine coastal ecosystems: The case of the Arcachon bay, France, *Progress in Oceanography*,  
972 201, 102740, <https://doi.org/10.1016/j.pocean.2022.102740>, 2022.
- 973 Liénart, C., Susperregui, N., Rouaud, V., Cavalheiro, J., David, V., Del Amo, Y., Duran, R.,  
974 Lauga, B., Monperrus, M., Pigot, T., Bichon, S., Charlier, K., and Savoye, N.: Dynamics of  
975 particulate organic matter in a coastal system characterized by the occurrence of marine  
976 mucilage – A stable isotope study, *Journal of Sea Research*, 116, 12–22,  
977 <https://doi.org/10.1016/j.seares.2016.08.001>, 2016.
- 978 Liénart, C., Savoye, N., Bozec, Y., Breton, E., Conan, P., David, V., Feunteun, E., Grangeré,  
979 K., Kerhervé, P., Lebreton, B., Lefebvre, S., L’Helguen, S., Mousseau, L., Raimbault, P.,  
980 Richard, P., Riera, P., Sauriau, P.-G., Schaal, G., Aubert, F., Aubin, S., Bichon, S., Boinet, C.,  
981 Bourasseau, L., Bréret, M., Caparros, J., Cariou, T., Charlier, K., Claquin, P., Cornille, V.,  
982 Corre, A.-M., Costes, L., Crispi, O., Crouvoisier, M., Czamanski, M., Del Amo, Y.,  
983 Derriennic, H., Dindinaud, F., Durozier, M., Hanquiez, V., Nowaczyk, A., Devesa, J.,  
984 Ferreira, S., Fournier, M., Garcia, F., Garcia, N., Geslin, S., Grossteffan, E., Gueux, A.,  
985 Guillaudeau, J., Guillou, G., Joly, O., Lachaussée, N., Lafont, M., Lamoureux, J., Lecuyer, E.,  
986 Lehodey, J.-P., Lemeille, D., Leroux, C., Macé, E., Maria, E., Pineau, P., Petit, F., Pujo-Pay,  
987 M., Rimelin-Maury, P., and Sultan, E.: Dynamics of particulate organic matter composition in  
988 coastal systems: A spatio-temporal study at multi-systems scale, *Progress in Oceanography*,  
989 156, 221–239, <https://doi.org/10/gb27ss>, 2017.
- 990 Liénart, C., Savoye, N., David, V., Ramond, P., Rodriguez Tress, P., Hanquiez, V., Marieu,  
991 V., Aubert, F., Aubin, S., Bichon, S., Boinet, C., Bourasseau, L., Bozec, Y., Bréret, M.,  
992 Breton, E., Caparros, J., Cariou, T., Claquin, P., Conan, P., Corre, A.-M., Costes, L.,  
993 Crouvoisier, M., Del Amo, Y., Derriennic, H., Dindinaud, F., Duran, R., Durozier, M.,  
994 Devesa, J., Ferreira, S., Feunteun, E., Garcia, N., Geslin, S., Grossteffan, E., Gueux, A.,  
995 Guillaudeau, J., Guillou, G., Jolly, O., Lachaussée, N., Lafont, M., Lagadec, V., Lamoureux,  
996 J., Lauga, B., Lebreton, B., Lecuyer, E., Lehodey, J.-P., Leroux, C., L’Helguen, S., Macé, E.,  
997 Maria, E., Mousseau, L., Nowaczyk, A., Pineau, P., Petit, F., Pujo-Pay, M., Raimbault, P.,  
998 Rimmelin-Maury, P., Rouaud, V., Sauriau, P.-G., Sultan, E., and Susperregui, N.: Dynamics  
999 of particulate organic matter composition in coastal systems: Forcing of spatio-temporal  
1000 variability at multi-systems scale, *Progress in Oceanography*, 162, 271–289,  
1001 <https://doi.org/10.1016/j.pocean.2018.02.026>, 2018.
- 1002 Liénart, C., Savoye, N., Conan, P., David, V., Barbier, P., Bichon, S., Charlier, K., Costes, L.,  
1003 Derriennic, H., Ferreira, S., Gueux, A., Hubas, C., Maria, E., and Meziane, T.: Relationship  
1004 between bacterial compartment and particulate organic matter (POM) in coastal systems: An  
1005 assessment using fatty acids and stable isotopes, *Estuarine, Coastal and Shelf Science*, 239,  
1006 106720, <https://doi.org/10.1016/j.ecss.2020.106720>, 2020.
- 1007 Lowe, A. T., Galloway, A. W. E., Yeung, J. S., Dethier, M. N., and Duggins, D. O.: Broad  
1008 sampling and diverse biomarkers allow characterization of nearshore particulate organic  
1009 matter, *Oikos*, 123, 1341–1354, <https://doi.org/10.1111/oik.01392>, 2014.
- 1010 Lu, L., Cheng, H., Pu, X., Wang, J., Cheng, Q., and Liu, X.: Identifying organic matter  
1011 sources using isotopic ratios in a watershed impacted by intensive agricultural activities in  
1012 Northeast China, *Agriculture, Ecosystems & Environment*, 222, 48–59,  
1013 <https://doi.org/10.1016/j.agee.2015.12.033>, 2016.



- 1014 Marshall, D. A., La Peyre, M. K., Palmer, T. A., Guillou, G., Sterba-Boatwright, B. D.,  
1015 Beseres Pollack, J., and Lebreton, B.: Freshwater inflow and responses from estuaries across a  
1016 climatic gradient: An assessment of northwestern Gulf of Mexico estuaries based on stable  
1017 isotopes, *Limnology and Oceanography*, 66, 3568–3581, <https://doi.org/10.1002/lno.11899>,  
1018 2021.
- 1019 McCorkle, E. P., Berhe, A. A., Hunsaker, C. T., Johnson, D. W., McFarlane, K. J., Fogel, M.  
1020 L., and Hart, S. C.: Tracing the source of soil organic matter eroded from temperate forest  
1021 catchments using carbon and nitrogen isotopes, *Chemical Geology*, 445, 172–184,  
1022 <https://doi.org/10.1016/j.chemgeo.2016.04.025>, 2016.
- 1023 Michener, R. H. and Kaufman, L.: *Stable Isotope Ratios as Tracers in Marine Food Webs: An*  
1024 *Update*, 1st ed., edited by: Michener, R. and Lajtha, K., Wiley,  
1025 <https://doi.org/10.1002/9780470691854.ch9>, 2007.
- 1026 Middelburg, J. J. and Herman, P. M. J.: Organic matter processing in tidal estuaries, *Marine*  
1027 *Chemistry*, 106, 127–147, <https://doi.org/10.1016/j.marchem.2006.02.007>, 2007.
- 1028 Miller, R. J., Page, H. M., and Brzezinski, M. A.:  $\delta^{13}\text{C}$  and  $\delta^{15}\text{N}$  of particulate organic  
1029 matter in the Santa Barbara Channel: drivers and implications for trophic inference, *Marine*  
1030 *Ecology Progress Series*, 474, 53–66, <https://doi.org/10.3354/meps10098>, 2013.
- 1031 Minaudo, C., Meybeck, M., Moatar, F., Gassama, N., and Curie, F.: Eutrophication mitigation  
1032 in rivers: 30 years of trends in spatial and seasonal patterns of biogeochemistry of the Loire  
1033 River (1980–2012), *Biogeosciences*, 12, 2549–2563, [https://doi.org/10.5194/bg-12-2549-](https://doi.org/10.5194/bg-12-2549-2015)  
1034 2015, 2015.
- 1035 Minaudo, C., Moatar, F., Coynel, A., Etcheber, H., Gassama, N., and Curie, F.: Using recent  
1036 high-frequency surveys to reconstitute 35 years of organic carbon variations in a eutrophic  
1037 lowland river, *Environ Monit Assess*, 188, 41, <https://doi.org/10.1007/s10661-015-5054-9>,  
1038 2016.
- 1039 Ogrinc, N., Markovics, R., Kanduč, T., Walter, L. M., and Hamilton, S. K.: Sources and  
1040 transport of carbon and nitrogen in the River Sava watershed, a major tributary of the River  
1041 Danube, *Applied Geochemistry*, 23, 3685–3698,  
1042 <https://doi.org/10.1016/j.apgeochem.2008.09.003>, 2008.
- 1043 O’Leary, M. H.: Carbon isotope fractionation in plants, *Phytochemistry*, 20, 553–567,  
1044 [https://doi.org/10.1016/0031-9422\(81\)85134-5](https://doi.org/10.1016/0031-9422(81)85134-5), 1981.
- 1045 Onstad, G. D., Canfield, D. E., Quay, P. D., and Hedges, J. I.: Sources of particulate organic  
1046 matter in rivers from the continental usa: lignin phenol and stable carbon isotope  
1047 compositions, *Geochimica et Cosmochimica Acta*, 64, 3539–3546,  
1048 [https://doi.org/10.1016/S0016-7037\(00\)00451-8](https://doi.org/10.1016/S0016-7037(00)00451-8), 2000.
- 1049 Parnell, A. C., Phillips, D. L., Bearhop, S., Semmens, B. X., Ward, E. J., Moore, J. W.,  
1050 Jackson, A. L., Grey, J., Kelly, D. J., and Inger, R.: Bayesian stable isotope mixing models,  
1051 *Environmetrics*, 24, 387–399, <https://doi.org/10.1002/env.2221>, 2013.
- 1052 Perdue, E. M. and Koprivnjak, J.-F.: Using the C/N ratio to estimate terrigenous inputs of  
1053 organic matter to aquatic environments, *Estuarine, Coastal and Shelf Science*, 73, 65–72,  
1054 <https://doi.org/10.1016/j.ecss.2006.12.021>, 2007.



- 1055 Phillips, D. L., Inger, R., Bearhop, S., Jackson, A. L., Moore, J. W., Parnell, A. C., Semmens,  
1056 B. X., and Ward, E. J.: Best practices for use of stable isotope mixing models in food-web  
1057 studies, *Can. J. Zool.*, 92, 823–835, <https://doi.org/10.1139/cjz-2014-0127>, 2014.
- 1058 Polsenaere, P., Savoye, N., Etcheber, H., Canton, M., Poirier, D., Bouillon, S., and Abril, G.:  
1059 Export and degassing of terrestrial carbon through watercourses draining a temperate  
1060 podzolized catchment, *Aquat Sci*, 75, 299–319, <https://doi.org/10.1007/s00027-012-0275-2>,  
1061 2013.
- 1062 Pradhan, U. K., Wu, Y., Wang, X., Zhang, J., and Zhang, G.: Signals of typhoon induced  
1063 hydrologic alteration in particulate organic matter from largest tropical river system of Hainan  
1064 Island, South China Sea, *Journal of Hydrology*, 534, 553–566,  
1065 <https://doi.org/10.1016/j.jhydrol.2016.01.046>, 2016.
- 1066 Regnier, P., Friedlingstein, P., Ciais, P., Mackenzie, F. T., Gruber, N., Janssens, I. A.,  
1067 Laruelle, G. G., Lauerwald, R., Luyssaert, S., Andersson, A. J., Arndt, S., Arnosti, C., Borges,  
1068 A. V., Dale, A. W., Gallego-Sala, A., Godd eris, Y., Goossens, N., Hartmann, J., Heinze, C.,  
1069 Ilyina, T., Joos, F., LaRowe, D. E., Leifeld, J., Meysman, F. J. R., Munhoven, G., Raymond,  
1070 P. A., Spahni, R., Suntharalingam, P., and Thullner, M.: Anthropogenic perturbation of the  
1071 carbon fluxes from land to ocean, *Nature Geosci*, 6, 597–607,  
1072 <https://doi.org/10.1038/ngeo1830>, 2013.
- 1073 Rousseeuw, P. J.: Silhouettes: A graphical aid to the interpretation and validation of cluster  
1074 analysis, *Journal of Computational and Applied Mathematics*, 20, 53–65,  
1075 [https://doi.org/10.1016/0377-0427\(87\)90125-7](https://doi.org/10.1016/0377-0427(87)90125-7), 1987.
- 1076 Sarma, V. V. S. S., Krishna, M. S., Prasad, V. R., Kumar, B. S. K., Naidu, S. A., Rao, G. D.,  
1077 Viswanadham, R., Sridevi, T., Kumar, P. P., and Reddy, N. P. C.: Distribution and sources of  
1078 particulate organic matter in the Indian monsoonal estuaries during monsoon, *Journal of*  
1079 *Geophysical Research: Biogeosciences*, 119, 2095–2111,  
1080 <https://doi.org/10.1002/2014JG002721>, 2014.
- 1081 Sato, T., Miyajima, T., Ogawa, H., Umezawa, Y., and Koike, I.: Temporal variability of  
1082 stable carbon and nitrogen isotopic composition of size-fractionated particulate organic matter  
1083 in the hypertrophic Sumida River Estuary of Tokyo Bay, Japan, *Estuarine, Coastal and Shelf*  
1084 *Science*, 68, 245–258, <https://doi.org/10.1016/j.ecss.2006.02.007>, 2006.
- 1085 Savoye, N., Aminot, A., Tr eguer, P., Fontugne, M., Naulet, N., and K erouel, R.: Dynamics of  
1086 particulate organic matter d15N and d13C during spring phytoplankton blooms in a  
1087 macrotidal ecosystem (Bay of Seine, France), *Marine Ecology Progress Series*, 255, 27–41,  
1088 <https://doi.org/10.3354/meps255027>, 2003.
- 1089 Savoye, N., David, V., Morisseau, F., Etcheber, H., Abril, G., Billy, I., Charlier, K., Oggian,  
1090 G., Derriennic, H., and Sautour, B.: Origin and composition of particulate organic matter in a  
1091 macrotidal turbid estuary: The Gironde Estuary, France, *Estuarine, Coastal and Shelf Science*,  
1092 108, 16–28, <https://doi.org/10.1016/j.ecss.2011.12.005>, 2012.
- 1093 Sigman, D. M., DiFiore, P. J., Hain, M. P., Deutsch, C., Wang, Y., Karl, D. M., Knapp, A. N.,  
1094 Lehmann, M. F., and Pantoja, S.: The dual isotopes of deep nitrate as a constraint on the cycle  
1095 and budget of oceanic fixed nitrogen, *Deep Sea Research Part I: Oceanographic Research*  
1096 *Papers*, 56, 1419–1439, <https://doi.org/10.1016/j.dsr.2009.04.007>, 2009.



- 1097 Souissi, S., Yahia-Kéfi, O. D., and Yahia, M. N. D.: Spatial characterization of nutrient  
1098 dynamics in the Bay of Tunis (south-western Mediterranean) using multivariate analyses:  
1099 consequences for phyto- and zooplankton distribution, *Journal of Plankton Research*, 22,  
1100 2039–2059, <https://doi.org/10.1093/plankt/22.11.2039>, 2000.
- 1101 Sun, X., Fan, D., Cheng, P., Hu, L., Sun, X., Guo, Z., and Yang, Z.: Source, transport and fate  
1102 of terrestrial organic carbon from Yangtze River during a large flood event: Insights from  
1103 multiple-isotopes ( $\delta^{13}\text{C}$ ,  $\delta^{15}\text{N}$ ,  $\Delta^{14}\text{C}$ ) and geochemical tracers, *Geochimica et*  
1104 *Cosmochimica Acta*, 308, 217–236, <https://doi.org/10/gn8qs5>, 2021.
- 1105 Turner, R. E., Milan, C. S., Swenson, E. M., and Lee, J. M.: Peak chlorophyll a concentrations  
1106 in the lower Mississippi River from 1997 to 2018, *Limnology and Oceanography*, n/a,  
1107 <https://doi.org/10/gpjm83>, 2022.
- 1108 Veyssy, E., Etcheber, H., Lin, R. G., Buat-Menard, P., and Maneux, E.: Seasonal variation  
1109 and origin of Particulate Organic Carbon in the lower Garonne River at La Reole  
1110 (southwestern France), *Hydrobiologia*, 391, 113–126,  
1111 <https://doi.org/10.1023/A:1003520907962>, 1998.
- 1112 Wang, X., Chen, Y., Yuan, Q., Xing, X., Hu, B., Gan, J., Zheng, Y., and Liu, Y.: Effect of  
1113 river damming on nutrient transport and transformation and its countermeasures, *Frontiers in*  
1114 *Marine Science*, 9, 2022.
- 1115 Wang, Y., Song, J., Duan, L., Yuan, H., Li, X., Li, N., Zhang, Q., Liu, J., and Ren, C.:  
1116 Combining sterols with stable carbon isotope as indicators for assessing the organic matter  
1117 sources and primary productivity evolution in the coastal areas of the East China Sea,  
1118 *Continental Shelf Research*, 223, 104446, <https://doi.org/10.1016/j.csr.2021.104446>, 2021.
- 1119 Yan, X., Yang, J.-Y. T., Xu, M. N., Wang, H., Dai, M., and Kao, S.-J.: Nitrogen isotope  
1120 constraint on the zonation of multiple transformations between dissolved and particulate  
1121 organic nitrogen in the Changjiang plume, *Science of The Total Environment*, 818, 151678,  
1122 <https://doi.org/10.1016/j.scitotenv.2021.151678>, 2022.
- 1123 Yu, F., Zong, Y., Lloyd, J. M., Huang, G., Leng, M. J., Kendrick, C., Lamb, A. L., and Yim,  
1124 W. W.-S.: Bulk organic  $\delta^{13}\text{C}$  and C/N as indicators for sediment sources in the Pearl River  
1125 delta and estuary, southern China, *Estuarine, Coastal and Shelf Science*, 87, 618–630,  
1126 <https://doi.org/10.1016/j.ecss.2010.02.018>, 2010.
- 1127 Zhang, Y., Meng, X., Bai, Y., Wang, X., Xia, P., Yang, G., Zhu, Z., and Zhang, H.: Sources  
1128 and features of particulate organic matter in tropical small mountainous rivers (SW China)  
1129 under the effects of anthropogenic activities, *Ecological Indicators*, 125, 107471,  
1130 <https://doi.org/10.1016/j.ecolind.2021.107471>, 2021.
- 1131
- 1132